Bull. astr. Soc. India (1981) 9, 181–213.

Role of scattering in emergent planetary radiation

R. K. Bhatia and K. D. Abhyankar *Centre of Advanced Study in Astronomy, Osmania University, Hyderabad 500 007*

Received 1981 July 10

Abstract. Starting from the basic concepts, the role played by multiple scattering in modifying the intensity and polarization of radiation incident on a planetary atmosphere is brought out. Formation of spectral lines in such an atmosphere is discussed in detail. Various ground-based methods of observation are given and the spectroscopic observational data for Jupiter and Venus reviewed till 1981. Areas which require further attention are identified. Results of absorption and polarization line profiles, computed by us for a semi-infinite Rayleigh scattering atmosphere, are presented for two phase angles of 5° and 87°.

Key words : scattering—planetary radiation—spectral lines.

1. Introduction

Scattering is of fundamental importance in deciphering the information content of the emergent radiation from a planetary atmosphere. In this review an attempt has been made to present a complete and coherent picture of its role.

Scattering, whether at the macroscopic or microscopic level, involves a change in the direction of motion of either one or both of the two colliding bodies due to their interaction. Familiar examples at the macroscopic level are from astronomy, *e.g.*, change in the direction of a comet due to its interaction with Jupiter. At the microscopic level we have the interaction of particles such as electron-electron, proton-electron, *etc.*, the interaction of photons with photons and that of radiation with particles; in this paper we shall be concerned with the last case of interaction between photons and molecular particles.

Let us imagine particles immersed in a unidirectional, monochromatic radiation field. It is important to note that scattering will take place only if the region constituted by these particles exhibits optical inhomogeneity, *i.e.*, the refractive index varies in space or time. Optical inhomogeneity can arise either due to the presence of foreign particles or due to the fluctuations in density if the medium is optically pure. If scattering takes place some radiation depending on the nature of the particles will be removed from this field due to a change in direction and will be effectively lost. In contrast to scattering,

whenever the energy represented by the radiation is truly lost, for example, when it is converted to other forms of energy, absorption is said to take place.. Scattering is characterised by the coefficient σ_ν and absorption by the coefficient κ_ν where the subscript ν denotes the frequency of the radiation. Frequently, both these coefficients are lumped together:

$$\chi_\nu = \kappa_\nu + \sigma_\nu. \qquad ...(1)$$

χ_ν is called the extinction coefficient and is defined by

$$dI_\nu = - I_\nu \chi_\nu \rho \, ds, \qquad ...(2)$$

where I_ν is the specific intensity of the incident radiation impinging on matter of unit cross-section and density ρ and dI_ν gives the change in intensity of the incident radiation on travelling a distance *ds*.

Two useful concepts, the optical depth τ_ν and the albedo for single scattering $\tilde{\omega}_\nu$, follow from these definitions. The optical depth is a measure of the degree of interaction of the radiation with matter of thickness *ds* and density ρ; it is defined by the relation

$$d\tau_\nu = \chi_\nu \rho \, ds. \qquad ...(3)$$

The total optical depth τ_ν of the matter is given by

$$\tau_\nu = \int_0^s \chi_\nu \rho \, ds. \qquad ...(4)$$

The albedo for single scattering $\tilde{\omega}_\nu$ is defined by

$$\tilde{\omega}_\nu = \frac{\sigma_\nu}{\sigma_\nu + \kappa_\nu}, \qquad ...(5)$$

which represents the probability of scattering of a photon as compared to its extinction. Evidently, when $\tilde{\omega}_\nu = 1$ there is no absorption; this is known as the conservative case of perfect scattering. When $\tilde{\omega}_\nu < 1$ we have non-conservative scattering. The concept of albedo is particularly useful when dealing with the problem of line-formation, because towards the centre of the line the absorption increases and the albedo becomes small. It is rare to find conservative scattering in nature. Even for scattering in the continuum the albedo is less than one.

If the frequency of the radiation changes because of scattering, it is termed incoherent scattering. Conversely, when there is no change of frequency, it is termed coherent. Broad energy levels make a major contribution towards incoherent scattering.

2. Angular dependence of scattering

Although we have stated that the direction in which the radiation is scattered depends on the nature of the particle, we have not specified it quantitatively; we do so now. Let radiation of specific intensity I_ν be incident on an element of matter of mass *dm*

in the direction defined by the elemental solid angle $d\omega'$. Then, the rate at which energy is scattered from this beam into a solid angle $d\omega$ can be represented by

$$\chi_\nu I_\nu d\omega \, dm \, \frac{p(\cos\Theta)}{4\pi} \, d\omega', \qquad \ldots(6)$$

where Θ is the angle between the incident and the scattered direction and p (cos Θ), known as the phase function, specifies the angular dependence of the scattered energy. For conservative scattering

$$\frac{1}{4\pi} \int_{4\pi} p(\cos\Theta) \, d\omega' = 1, \qquad \ldots(7)$$

i.e., the probability that the photon will be scattered in some direction is one. However when absorption is present the probability is not unity and then we write, for a frequency ν

$$\frac{1}{4\pi} \int_{4\pi} p(\cos\Theta) \, d\omega' = \tilde{\omega}_0, \qquad \ldots(8)$$

where $\tilde{\omega}_0$ is the single scattering albedo we have already encontered; in general, $\tilde{\omega}_0 < 1$.

Different phase functions

The following are some of the phase functions commonly encountered in astrophysics (see, *e.g.*, van de Hulst 1980):

(i) Isotropic scattering

$$p(\cos\Theta) = \tilde{\omega}_0. \qquad \ldots(9)$$

(ii) Anisotropic scattering

$$p(\cos\Theta) = \tilde{\omega}_0(1 + a\cos\Theta) \qquad \ldots(10)$$

where $(-1 \leqslant a \leqslant 1)$.

(iii) Rayleigh scattering by particles of size less than that of the wavelength of the incident radiation

$$p(\cos\Theta) = \tfrac{3}{4}\,\tilde{\omega}_0(1 + \cos^2\Theta). \qquad \ldots(11)$$

(iv) Henyey-Greenstein phase function

$$p(\cos\Theta) = \frac{\tilde{\omega}_0(1 - g^2)}{(1 + g^2 - 2g\cos\Theta)^{3/2}}. \qquad \ldots(12)$$

(v) Mie scattering by aerosols or particles of size of the order of or greater than the wavelength of the incident radiation

$$p(\cos\Theta) = \sum_{l=0}^{\infty} \tilde{\omega}_l \, P_l(\cos\Theta) \qquad \ldots(13)$$

where P_l are the Legendre functions.

The asymmetry factor g in (iv) takes into account the departure from isotropic scattering. To a certain extent, this is attained by the factor 'a' in (ii), but (iv) is a more general representation where g is given by

$$g = \langle \cos \Theta \rangle = \tfrac{1}{2} \tilde{\omega}_0 \int_{-1}^{+1} p(\cos \Theta) \cos \Theta \, d(\cos \Theta). \qquad ...(14)$$

This is clearly the weighted mean of the cosine of the scattering angle. It is zero for isotropic scattering and approaches unity for particles such as aerosols which have a highly elongated forward scattering phase function. It is possible to have $g < 0$ for strongly backward scattering particles such as small metallic ones. Schematic scattering diagrams for these cases are shown in Figure 1.

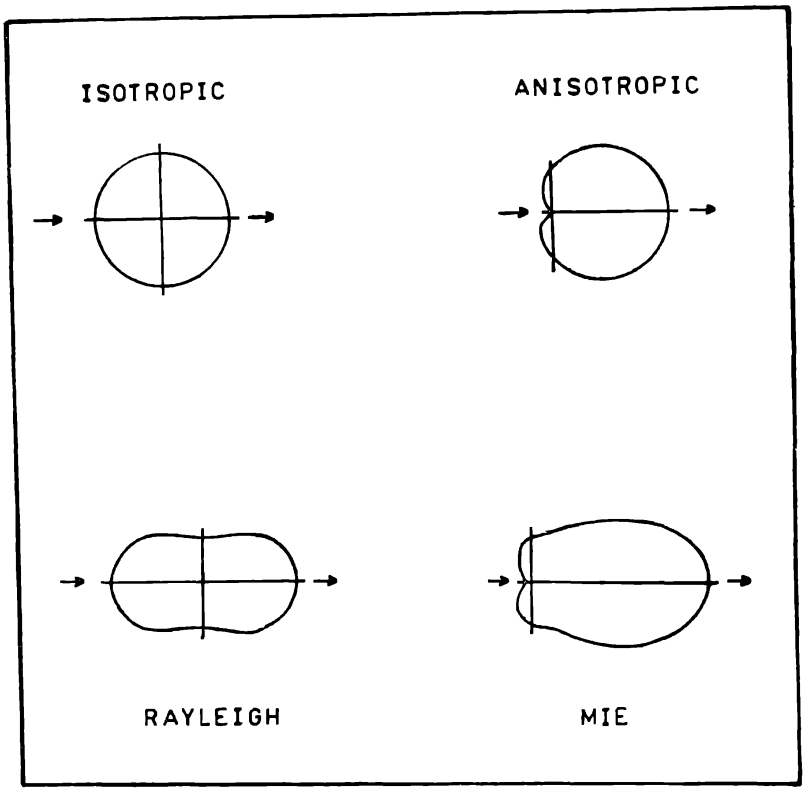

Figure 1. Schematic diagrams of typical phase functions.

3. Representation of polarization

The blueness of the sky is due to molecular scattering by the constituents of the atmosphere. Apart from the colour, there is another aspect to the scattered radiation, it is polarized, the degree of polarization depending on the point considered and its angular distance from the sun. To account for this, and also for polarization introduced by Mie scattering, we must consider I as a vector having the components (I, Q, U, V) which are known as Stokes parameters represented by a (4 × 1) column matrix (Chandrasekhar 1960, p. 24). Mathematically, the four parameters are given by the time averages

$$I = \langle E_l E_l^* + E_r E_r^* \rangle = \langle a_l^2 + a_r^2 \rangle \quad \ldots(15)$$

$$Q = \langle E_l E_l^* - E_r E_r^* \rangle = \langle a_l^2 - a_r^2 \rangle \quad \ldots(16)$$

$$U = \langle E_l E_r^* + E_r E_l^* \rangle = 2 \langle a_l a_r \cos (\epsilon_l - \epsilon_r) \rangle \quad \ldots(17)$$

$$V = i \langle E_l E_r^* - E_r E_l^* \rangle = 2 \langle a_l a_r \sin (\epsilon_l - \epsilon_r) \rangle \quad \ldots(18)$$

where

$$E_l = a_l \exp [+ i(wt - kz - \epsilon_l)] \quad \ldots(19)$$

$$E_r = a_r \exp (- i(wt - kz - \epsilon_r)] \quad \ldots(20)$$

are the components of the electric vector in any two mutually perpendicular directions, l and r, of a wave of frequency ν travelling in the positive z-direction. Here a_l and a_r are the amplitudes, ϵ_l and ϵ_r the phases, t the time, $i = \sqrt{-1}$, k the wave number $2\pi/\lambda$ and the asterisk denotes the complex conjugate.

For completely polarised radiation, $\epsilon_l - \epsilon_r$ is a constant and the electric vector represented by the two components E_l and E_r will, in general, describe an ellipse in space. To define this ellipse we need to specify its ellipticity and its orientation in space, *i.e.*, the angle the major axis makes with the l-direction.

The ellipticity can be defined by an angle β in terms of the semi-major and semi-minor axes a and b so that

$$\tan \beta = \pm b/a, \quad [-\pi/4 \leqslant \beta \leqslant \pi/4]. \quad \ldots(21)$$

In terms of the Stokes parameters, β is given by

$$\sin 2\beta = V/(Q^2 + U^2 + V^2)^{1/2}, \quad \ldots(22)$$

which, since

$$I = (Q^2 + U^2 + V^2)^{1/2}, \quad \ldots(23)$$

(cf. equations (15) – (18)), can also be written as

$$\sin 2\beta = V/I. \quad \ldots(24)$$

The sign of $\tan \beta$ determines the sense of rotation of the ellipse. For example, when $\tan \beta = 1$, the electric vector moves clockwise as viewed by an observer looking in the direction of propagation, the resulting polarization is called right-handed polarization; when $\tan \beta = -1$, the electric vector moves in an anticlockwise direction and the polarization is called left-handed. For $\tan \beta = 0$, we have linear polarization. The angle χ between the major axis and the direction l is given by (see Figure 2)

$$\tan 2\chi = U/Q. \quad \ldots(25)$$

For unpolarized or natural radiation the Stokes components Q and V are zero. Any radiation will be a mixture of polarized and unpolarized radiation. We have seen that the intensity of polarized radiation is given by

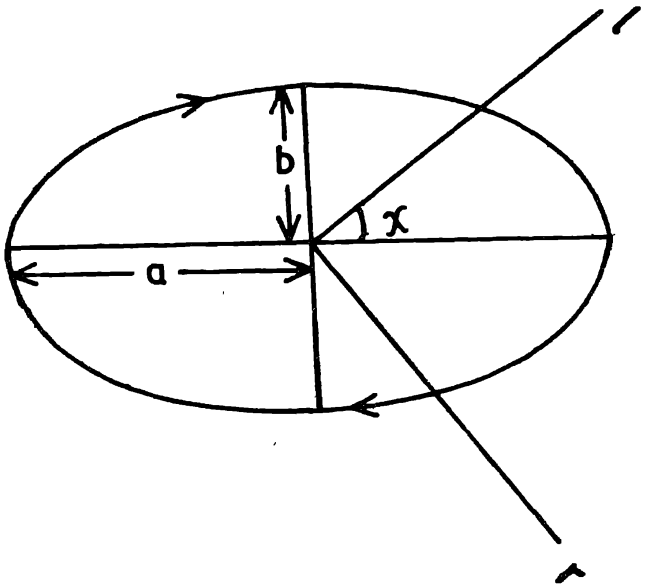

Figure 2. Representation of elliptical polarization.

$$I_{\rm pol} = (Q^2 + U^2 + V^2)^{1/2}. \qquad ...(26)$$

If I is the total intensity of the mixture, the degree of polarization is given by

$$p = \frac{I_{\rm pol}}{I} = \frac{(Q^2 + U^2 + V^2)^{1/2}}{I}. \qquad ...(27)$$

Evidently, when $I = I_{\rm pol}$ the radiation is completely polarized. The degree of circular polarization is given by

$$p^{\rm c} = \frac{I^{\rm c}_{\rm pol}}{I} = \frac{V}{I} \qquad ...(28)$$

and that of linear polarized by

$$p^{l} = \frac{I^{l}_{\rm pol}}{I} = \frac{(Q^2 + U^2)^{1/2}}{I}. \qquad ...(29)$$

Frequently, the intensities are expressed in terms of $I_{\parallel}$ and $I_{\perp}$ the intensities respectively parallel and perpendicular to the scattering plane defined by the incident and scattered beams. In that case, we can define one more quantity

$$P = \frac{I_{\perp} - I_{\parallel}}{I_{\perp} + I_{\parallel}}. \qquad ...(30)$$

It is this quantity which is normally measured by observers. However, it does not give the complete picture of polarization.

When I is considered as a vector, the angular dependence of scattering is given by a matrix, called the phase matrix. For Rayleigh scattering the phase matrix is given by

$$P(\cos\Theta) = \begin{bmatrix} \frac{3}{4}(1+\cos^2\Theta) - \frac{3}{4}\sin^2\Theta & 0 & 0 \\ -\frac{3}{4}\sin^2\frac{3}{4}\Theta & \frac{3}{4}(1+\cos^2\Theta) & 0 & 0 \\ 0 & 0 & \frac{3}{2}\cos\Theta & 0 \\ 0 & 0 & 0 & \frac{3}{2}\cos\Theta \end{bmatrix} \quad \ldots(31)$$

For Mie scattering, the phase matrix is given by

$$\tilde{P} = K\tilde{F},$$

where K is a constant and $\tilde{F}$, known as the transformation matrix, is given by the following 4 × 4 matrix (Hansen & Travis 1974; van de Hulst 1957):

$$\begin{bmatrix} \frac{1}{2}(S_1S_1^* + S_2S_2^*) & \frac{1}{2}(S_1S_1^* - S_2S_2^*) & 0 & 0 \\ \frac{1}{2}(S_1S_1^* - S_2S_2^*) & \frac{1}{2}(S_1S_1^* + S_2S_2^*) & 0 & 0 \\ 0 & 0 & \frac{1}{2}(S_1S_2^* + S_2S_1^*) & \frac{i}{2}(S_1S_2^* - S_2S_1^*) \\ 0 & 0 & -\frac{i}{2}(S_1S_2^* - S_2S_1^*) & \frac{1}{2}(S_1S_2^* + S_2S_1^*) \end{bmatrix} \quad \ldots(32)$$

Here S_1 and S_2 are the elements of the scattering matrix whose form depends on the problem under consideration.

4. Multiple scattering

Our discussion till now has been confined to single scattering. It is evident that when radiation enters an atmosphere, the emergent radiation will undergo a number of scatterings, the probability being a function of the albedo and the optical depth of the atmosphere. In other words, if a particle has a high probability of absorption *i.e.* low albedo it will have undergone fewer scatterings before emerging and vice versa.

There are a variety of methods available for computing the intensity emergent from the atmosphere of any arbitrary optical thickness. An atmosphere bounded on two sides is considered finite, *e.g.*, the earth's atmosphere. On the other hand, an atmosphere bounded on one side only is semi-infinite, such as the sun's. We will only briefly mention the various methods used for obtaining the effect of multiple scattering; for details the reader is referred to the excellent exposition by Hansen & Travis (1974) (see also Irvine 1975).

The methods are :

(i) *invariant imbedding method* in which the change in reflection or transmission is studied when a layer of small optical thickness is added to the atmosphere;

(ii) the *extension* of the invariant imbedding method where the equation obtained from the principles of invariance gives, after differentiating and applying the necessary boundary conditions, non-linear integral equations which can be solved numerically. These give the so-called X- and Y-functions for finite atmospheres and H-functions for semi-infinite atmospheres;

(iii) the *spherical harmonics method* in which the intensity is expanded in terms of spherical harmonics;

(iv) the *method of discrete ordinates* in which the radiation field is divided into $m = 2n$ streams in m different directions. This gives m simultaneous equations in m unknowns which can be solved to give the emergent intensity;

(v) the *adding method* in which the atmosphere is built up layer-by-layer taking into account the reflection and transmission properties of the individual layers at each step. A useful modification of this method is to double the thickness of a layer at each step; this is called the *doubling method*;

(vi) the *successive order of scattering method* in which the intensity of each order of scattering is computed and the total intensity found by summing over all these orders,

(vii) expansion in eigenfunctions; and

(viii) the *Monte-Carto method* the use of which has become feasible with the availability of modern fast computers.

In most of these methods a plane parallel atmosphere is assumed. The reflected (or transmitted) intensity is computed in terms of the incident flux πF in the direction (μ_0, φ_0). The relevant formulas are (Chandrasekhar 1960, p. 20)

$$I_{\text{ref}}(\tau_1, \mu, \varphi) = \frac{F}{4\mu} S(\tau_1; \mu, \varphi; \mu_0, \varphi_0) \qquad \ldots(33)$$

$$I_{\text{trans}}(\tau_1, \mu, \varphi) = \frac{F}{4\mu} T(\tau_1; \mu, \varphi, \mu_0; \varphi_0). \qquad \ldots(34)$$

Here $I_{\text{ref}}(\tau_1; \mu, \varphi)$ and $I_{\text{trans}}(\tau_1; \mu, \varphi)$ are the reflected and transmitted intensities respectively in the direction (μ, φ) and S and T are the scattering and transmission functions; the factor 4μ in the denominator appears for mathematical convenience.

We now require to calculate S and T in the case of finite atmospheres, or S alone in the case of semi-infinite atmospheres. As an illustration, consider the semi-infinite case. First of all, we obtain from the principles of invariance an integral equation for S (Chandrasekhar 1960, p. 94) in terms of the phase function:

$$\left(\frac{1}{\mu} + \frac{1}{\mu_0}\right) S(\mu, \varphi; \mu_0, \varphi_0)$$

$$= p(\mu, \varphi; -\mu_0, \varphi_0) + \frac{1}{4\pi} \int_0^1 \int_0^{2\pi} p(\mu, \varphi; \mu'', \varphi'')\, S(\mu'', \varphi''; \mu_0, \varphi_0) \frac{d\mu''}{\mu''}\, d\varphi''$$

$$+ \frac{1}{4\pi} \int_0^1 \int_0^{2\pi} S(\mu, \varphi; \mu', \varphi')\, p(\mu', \varphi'; \mu_0, \varphi_0) \frac{d\mu'}{\mu'}\, d\varphi'$$

$$+ \frac{1}{(4\pi)^2} \int_0^{12} \int_0^{\pi} \int_0^1 \int_0^{2\pi} S(\mu, \varphi; \mu', \mu')\, p(\mu', \varphi'; \mu'', \varphi'')$$

$$\times S(\mu'', \varphi''; \mu_0, \varphi_0) \frac{d\mu'}{\mu'}\, d\varphi', \frac{d\mu''}{\mu''}\, d\varphi'' \qquad \ldots(35)$$

After substituting the expression for the required phase function, we obtain the following non-linear integral equations for $H(\mu)$:

$$H(\mu) = 1 + \mu H(\mu) \int_0^1 \frac{\Psi(\mu')\, H(\mu')\, d\mu'}{\mu + \mu'}, \qquad ...(36)$$

where $\Psi(\mu)$ is called the characteristic function. It is an even polynomial in μ satisfying the condition.

$$\int_0^1 \Psi(\mu)\, d\mu \leqslant \tfrac{1}{2}. \qquad ...(37)$$

The form of $\Psi(\mu)$ depends on the type of phase function employed. Equations (33) – (35) can be extended to include polarization in which case S and T have matrix forms. For example in the case of non-conservative Rayleigh scattering we obtain after a lot of involved mathematics the following expressions for the Stokes parameters, in terms of several H-functions (Lenoble 1970) :

$$\begin{aligned} I_l = \frac{3}{32}\tilde{\omega}_0 \frac{\mu_0}{\mu+\mu_0} \{&[\mu^2 H_1(\mu) + \sqrt{2}(1-\mu^2)\, H_3(\mu)\, [\mu_0^2 H_1(\mu_0) \\ &+ \sqrt{2}\,(1-\mu_0^2)\, H_3(\mu_0) + H_1(\mu_0)]] + [\mu^2 H_2(\mu) \\ &+ \sqrt{2}\,(1-\mu^2)\, H_4(\mu)\, [\mu_0^2 H_2(\mu_0) + \sqrt{2}\,(1-\mu^2) H_4(\mu_0) + H_2(\mu_0)]] \\ &- 4\mu\mu_0 \cos(\varphi_0 - \varphi)(1-\mu^2)^{1/2}(1-\mu_0^2)^{1/2} H^{(1)}(\mu)\, H^{(1)}(\mu_0) \\ &+ (\mu_0^2 - 1)\, \mu^2 \cos 2(\varphi_0 - \varphi)\, H^{(2)}(\mu)\, H^{(2)}(\mu_0)]\} F, \end{aligned} \qquad ...(38)$$

$$\begin{aligned} I_r = \frac{3}{32}\tilde{\omega}_0 \frac{\mu_0}{\mu+\mu_0} \{&[H_1(\mu)\, [\mu_0^2 H_1(\mu_0) + \sqrt{2}\,(1-\mu_0^2) H_3(\mu_0) \\ &+ H_1(\mu_0)]] + [H_2(\mu)[\mu_0^2 H_2(\mu_0) + \sqrt{2}(1+\mu_0^2 H_4(\mu_0) \\ &+ H_2(\mu_0)]] - (\mu_0^2 - 1)\cos 2(\varphi_0 - \varphi)\, H^{(2)}(\mu)\, H^{(2)}(\mu_0)\} F, \end{aligned} \qquad ...(39)$$

$$\begin{aligned} U = \frac{3}{16}\tilde{\omega}_0 \frac{\mu_0}{\mu+\mu_0} &[2\mu_0 \sin(\varphi_0 - \varphi)(1-\mu^2)^{1/2}(1-\mu_0^2)^{1/2} H^{(1)}(\mu) H^{(1)}(\mu_0) \\ &+ \mu(1-\mu_0^2)\sin 2(\varphi_0 - \varphi) H^{(2)}(\mu) H^{(2)}(\mu_0)]\, F, \end{aligned} \qquad ...(40)$$

where $H^{(1)}$ and $H^{(2)}$ are the H-functions for $\Psi^{(1)}(\mu) = \frac{3}{8}\tilde{\omega}_0(1 + 2\mu^2)(1 - \mu^2)$ and $\Psi^{(2)}(\mu) = (3/16)\,\tilde{\omega}_0(1 + \mu^2)^2$, respectively and H_1, H_2, H_3, H_4 are the elements of the matrix $\tilde{H}$-function corresponding to the matrix $\tilde{\Psi}$ function with elements $\Psi_1(\mu) = \frac{3}{8}\tilde{\omega}_0\,(\mu^4 + 1)$, $\Psi_2(\mu) = \Psi_3(\mu) = \frac{3}{8}\tilde{\omega}_0\,\sqrt{2}\mu^2(1 - \mu^2)$, $\Psi_4(\mu) = \frac{3}{8}\tilde{\omega}_0(1 - \mu^2)^2$.

5. Basic theory for spectral lines

(a) *The line profile* : It gives the variation of intensity (or polarization) as a function of frequency within the line. This in turn depends among other things on the absorption profile, which gives the variation of absorption coefficient along the line in terms of the absorption coefficient at the centre. Depending on the pressure, the types of absorption profile chosen are : Doppler (low pressure),

Voigt (intermediate pressure), Lorentz (high pressure) or Galatry (very high pressure causing collision narrowing); *cf.* Dicke (1953), James (1969). All these profiles are centrally symmetric.

The expression for the Lorentz profile is

$$k_\nu = k_0(1 + x^2)^{-1} \qquad ...(41)$$

where $x = (\nu - \nu_0)/\alpha_L$, α_L being the Lorentz half-width of the line and ν_0 the frequency at the line centre. When scattering is present, this is expressed in terms of the albedo as

$$\tilde{\omega}_\nu = \left[1 + \frac{(1 - \tilde{\omega}_0)}{(1 + x^2)}\right]^{-1}, \qquad ...(42)$$

where $\tilde{\omega}_0$ is the albedo at the line centre. Further, if we wish to take into account the absorption in the continuum (usually small) we must write

$$\tilde{\omega}_\nu = \frac{\sigma_\nu}{\sigma_\nu + k_\nu + k_c} = \left[\frac{1}{\tilde{\omega}_\nu} + \frac{1}{\tilde{\omega}_c} - 1\right]^{-1} \qquad ...(43)$$

or

$$\tilde{\omega}'_\nu = \left[\frac{1 - \tilde{\omega}_0}{\tilde{\omega}_0(1 + x^2)} + \frac{1}{\tilde{\omega}_c}\right]^{-1}, \qquad ...(44)$$

where k_c is the absorption in the continuum. The appropriate equation of transfer is solved to obtain S as a function of $\tilde{\omega}_\nu$ and then the line profile is given by the use of equation (33) or (34) as

$$I_\nu = \frac{S(\tilde{\omega}_\nu)}{S(\tilde{\omega}_c)}. \qquad ...(45)$$

When polarization is taken into account we can obtain I_ν, $I_{\nu_\parallel}$, $I_{\nu_\perp}$ and p_ν, p_ν^c, p_ν^l or P_ν by the same procedure.

(b) *The equivalent width* : The equivalent width is a measure of the amount of light blacked out by the absorption line. It is given by

$$W = \int_{\text{line}} \frac{(I_c - I_\nu)}{I_c}\, d\nu \text{ (in terms of intensity)}, \qquad ...(46)$$

and

$$W = \int_{\text{line}} \frac{(F_c - F_\nu)}{F_c}\, d\nu \text{ (in terms of flux)}, \qquad ...(47)$$

where the subscript c denotes the continuum. In the latter case it is convenient to use Horak's (1950) method of Gaussian and Chebichev quadratures. For example, the points in the latitude-longitude grid for two phase angles of 5° and 87° are shown in Figure 3.

6. Application to planetary atmospheres

Our aim in studying planetary atmospheres is to determine, among other things, their (i) chemical composition, (ii) abundances, (iii) structure (the run of pressure,

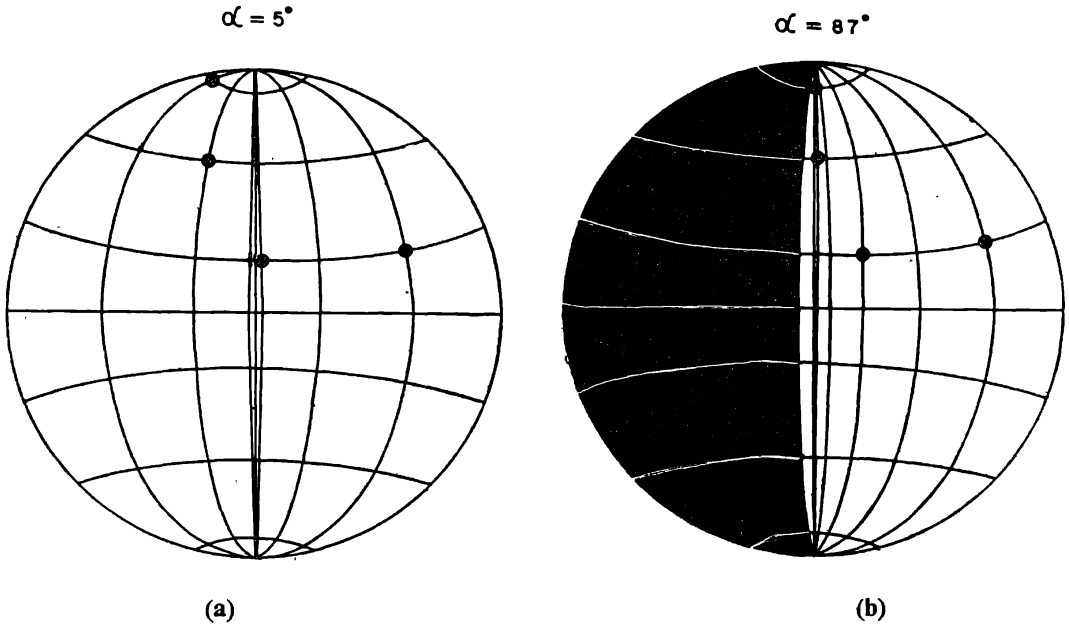

Figure 3. (a) and (b). Points in the latitude-longitude grid for cubature for two phase angles. Note the symmetry with respect to the equator. The shaded area is the region not visible.

temperature, *etc.* with height), and (iv) cloud structure. The determination of chemical composition and abundances is of special significance, especially for the Jovian planets, because they are supposed to have the same chemical composition as that of the primordial nebula from which the solar system is thought to have evolved (Newburn & Gilkis 1973). Comparison of their abundances with that of solar abundances throws light on the same problem. As we shall see, scattering has a direct bearing on how we obtain these parameters.

What we observe from the planetary atmospheres is the intensity at various points on the disk, and quite often the integrated flux for the whole disk at various phases, the phase angle being defined as the planetocentric elongation of the earth from the sun. However, due to atmospheric seeing, guiding errors and the finite aperture of the instrument employed, it is not possible to observe a particular point on the disk, the observations are always an average over a small region. We have seen that the intensity of the scattered radiation for an incident flux F, depends on : (i) the angle between the incident and the scattered direction and (ii) the type of phase function for the scattering particles. Therefore, to decide about the nature of particles, we need observations at different angular configurations. To do so we can, as already mentioned, observe the intensity of different points on the disk of the planet. In addition, we can observe the change of (i) intensity at a point, say the centre, on the disk, and (ii) the integrated flux from the whole planet, with phase angle. In the first case we can study the so called centre-to-limb variation of the intensity in the continuum or of the equivalent widths of the absorption lines. In both cases we can study the change in the equivalent widths as functions of phase angle.

In the continuum, either the change in intensity, or the integrated flux (or magnitude, or Bond-albedo, or spherical albedo) can be studied. Another powerful tool is

polarization which again can be studied at a particular phase angle, either (i) in the continuum or (ii) along an absorption line; further, its change with phase angle can be studied. All these studies can be made with respect to the wavelength. Lately, *in-situ* measurements by space probes have supplemented ground based observations of these kinds.

7. Studies of the Venus and Jupiter atmospheres

That the atmosphere of Jupiter should be gaseous was pointed out as early as the 1870s by Vogel who inspected the spectrum visually (see *e.g.* Kiess, Corliss & Kiess 1960). Later observers, using different techniques, identified gases like CH_4, NH_3, H_2, He, CH_3D, C_2H_6, & C_2H_2, and others (see *e.g.* Baum & Code 1953 and Beer & Taylor 1973). However, the major constituent of Jupiter's atmosphere is H_2 which is observed only as weak lines of the (3-0) and (4-0) bands. On Venus CO_2 in gaseous form was first identified by Adams & Dunham (1932) from spectroscopic observations; we now know that this is the major constituent of the Cytherean atmosphere. Later observations have revealed the presence in small quantities of substances like N_2, HCL, H_2O, HF, CO and H_2SO_4 (Young 1974). Several approaches can be made for the study of the spectra of Jupiter and Venus as discussed below.

(a) *The behaviour of equivalent widths*: Hess (1953) in his pioneering work investigated the variation in the strength of absorption of the 6190 Å CH_4 band and the 6441 Å NH_3 band across the disks of Jupiter and Saturn. For Jupiter he came up with the surprising result that the equivalent widths of the two bands decreased slightly towards the limb along the equator. This study was made at a dispersion of 43 Å mm^{-1}. Later investigators, using higher dispersions, found essentially the same change in absorption (Munch & Younkin 1964, Teifel 1966, 1969, Owen 1969, Moroz & Cruikshank 1969, Avramchuk 1970, Avery *et al.* 1974). The lone work of dissent has been that of Boyce (1968) who found the reverse trend.

The other bands of CH_4 at 7250, 8860, and 9900 Å exhibit the same behaviour (Teifel 1976). Moroz & Cruikshank (1969) and Binder (1972) observed the strong 1.1μ NH_3 band and found similar behaviour. Along the equator at $0.73R$, where R is the radius of the planetary disk, they found that the absorption is less by a factor of 0.7 than at the centre. As McElroy (1969) has pointed out, these observations are incompatible with a reflecting-layer model for the atmosphere in which absorption takes place in the gas overlying a Lambertian reflecting surface, for the reason that in such an atmosphere the strength of absorption should increase as one goes towards the limb because of the larger amount of gas encountered. Nevertheless, this model is useful as a first approximation for the centre of the disk. Margolis & Fox (1969a, b) have used this model for deriving abundances and the rotational temperature for Jupiter.

The latitudinal variation of some of these bands has also been studied. The 6190, 7250, and 8860 Å CH_4 bands first show an increase in absorption with latitude and then a decrease towards the poles (Owen & Westphal 1972, Teifel 1966, 1969, Avery *et al.* 1974). A similar trend is observed in photographs of Jupiter taken with narrow band interference filters (Owen 1969, Owen & Mason 1969, Kuiper 1972, Minton 1972, Fountain 1972). In the 1.1 and 1.6μ NH_3 bands, Binder & McCarthy (1973) have observed an increase in absorption with latitude.

Individual lines have been studied in the 1.1μ CH_4 band by Walker & Hayes (1967) and Bergstralah (1973). For the equivalent widths of lines in the 1.1μ band, Walker & Hayes find a near constancy along the equator while Bergstralah finds a slight increase towards the limb. The narrow hydrogen quadrupole lines in the (4, 0) band at 6735 Å and in the (3, 0) band at 8150 Å have been observed by Carleton & Traub (1974), and Hunt & Bergstralah (1974, 1977). For the $S(1)$ lines of both the H_2 bands Carleton and Traub find the equivalent width to be slightly less (10 per cent) at the limb compared to that at the centre. Hunt & Bergstralah find a similar trend. However, Cochran (1977) finds the equivalent width of the $S(1)$–(4, 0) line to be nearly constant along the equator with a slight increase at the limb.

Since Jupiter's phase angle reaches a maximum value of only 12 deg., Venus is the planet for which the phase variation of the equivalent widths of line in the CO_2 bands have been well studied. The weakening of lines in the spectrum at large phase angles was first noticed by Kuiper (1952) and investigated by Chamberlain & Kuiper (1956). Later observations (Young 1972, Schorn *et al.* 1975, Barker & Macy 1977, Macy & Trafton 1977) point to an increase in equivalent width up to a phase angle of about 90 deg. and then a decrease.

Lastly, a number of authors have mentioned about temporal fluctuations of the equivalent widths and have taken care to have short observation times when studying spatial or phase variations. Efforts have been made to study this change by Teifel (1976), Young *et al.* (1973), Young & Margolis (1977) and Barker & Perry (1975).

(b) *Models* : A lot of effort has been directed toward the computation of line profiles taking scattering into account. Depending on the model chosen for the atmosphere, these efforts can be broadly classified into three categories.

(i) Finite or semi-infinite homogeneous atmosphere with different phase functions (Chamberlain 1965, 1970; Belton 1968, Lenoble 1968 , Belton *et al.* 1968, McElroy 1969; Pilcher & Kunkle 1976, Regas *et al.* 1975, Teifel 1976).

(ii) Semi-infinite atmosphere with Rayleigh phase matrix taking polarization into account (Lenoble 1970, Fymat 1974, Buriez *et al.* 1979).

(ii) Multi-layered atmospheres with or without aerosols (Danielson & Tomasko 1969, Hunt 1972a, b, Hunt 1973a, b, c,. Carleton & Traub 1974, Chamberlain & Smith 1970, Appelby & Blerkom 1975, Martin *et al.* 1976; Macy & Trafton 1976; Young & Kattawar 1976, Teifel 1977a; Kattawar & Young 1977, Young & Kattawar 1977, Hunt & Bergstralah 1977, Barker & Macy 1977, Cocharan 1977, Macy & Trafton 1977; Macy 1976; Smith *et al.* 1980; Sobolev 1972, Anikonov 1977).

From these studies it is seen that a number of models explain the observed variation of the line profiles across the planet's disk. The present trend seems to favour multi-layered models. However, these models introduce several arbitrary parameters; Teifel (1977b) has rightly emphasised the need for simple models.

(c) *The rotational temperature* : The earliest attempt at determining the rotational temperature for Venus was by Adel (1937) who from the prints published by Adams & Dunham concluded that the temperature must be greater than 320 K. Later, more attempts were made (Dunham 1949, Herzberg 1951) to determine the temperature,

but all made the assumption that the relative intensities of the lines were proportional to the relative populations N_J of the lower levels. Using the arguments of van de Hulst (1952), Chamberlain & Kuiper (1956) stressed that instead of the familiar linear dependence of the equivalent width of weak lines on the number of absorbing particles, there should be a square root dependence *i.e.*, $W \propto (N_J)^{1/2}$, in the optically thick atmosphere scattering isotropically. They applied this to the 7820 Å CO_2 band and derived a rotational temperature of 285 ± 9 K. However, Spinrad's (1962) analysis of some spectra showed that a linear law gave a better fit to the observations. Chamberlain (1965), on the basis of radiative transfer theory, again stressed the square-root dependence of the equivalent widths. On taking continuum absorption into acccount, McClathey (1967) discovered a linear dependence. Gray (1969) reanalysed Spinrad's data and found that a square-root dependence gave a better fit to the data. L.D.G. Young and her collaborators have been monitoring the CO_2 bands continuously for the past decade and have been using both the laws. We deal with their method quantitatively below.

The Boltzmann distribution of the rotational energy levels of a molecule at temperature T is given by (Goody 1964)

$$\frac{n(J)}{N} = \frac{w_J(2J+1)\exp(-E_r(J)/kT)}{Q_{\rm rot}}, \qquad \ldots(48)$$

where $n(J)$ = number of molecules in the Jth energy level,

N = total number of molecules *i.e.*, $\Sigma\, n(J)$,

w_J = nuclear weight factor,

$Q_{\rm rot}$ = rotational partition function,

$E_r = hcBJ(J+1)$, the rotational energy of the molecule in level J,

B = rotational constant.

It can be shown that (Boese *et al.* 1966) :

$$S(J) = \frac{S_{\rm band}\, J \exp[-hcBJ(J+1)/kT]}{Q_{\rm rot}}, \qquad \ldots(49)$$

where $S(J)$ and $S_{\rm band}$ represent the line intensity and band intensity, respectively. This expression holds for the P-branch. For a general expression which includes the R-branch, we have

$$S(m) = \frac{S_{\rm band}\, m \exp[-hcBm(m-1)/kT]}{Q_{\rm rot}}, \qquad \ldots(50)$$

where $m = J + 1$ for the R-branch, and $m = -J$ for the P-branch.

The equivalent width will depend on the line intensity. This variation is expressed in the form of a curve-of-growth. For weak lines

$$W = S^b \qquad \ldots(51)$$

i.e. a straight line of slope b in the log-log plot. The value of b depends on the model chosen; *e.g.*, $b = 0.5$ for Chamberlain's radiative transfer theory for an optically

thick atmosphere scattering isotropically, and $b = 1.0$ for a clear, non-scattering atmosphere. From equations (50) and (51) it follows that

$$\ln\left(\frac{W}{m^b}\right) = \ln(W_0) - \frac{hc\,Bm(m-1)\,b}{kT}\,, \qquad \ldots(52)$$

where W_0 is a constant used to determine the abundance (Young 1972). There are two ways in which the temperature can be determined:

(i) We assume that $b = 0.5$ and plot $\ln\left(\frac{W}{m^b}\right)$ versus $m\,(m-1)\,0.5$. The slope of this plot gives the temperature.

(ii) We do not assume that $b = 0.5$, but evaluate expression (52) for different values of T and make a least square fit. The value of T for which we get minimum standard deviation is the correct value. The slope of this line then gives b. This value of the slope is used to recompute the curve of growth to find the new T. This iteration is continued till both T and b do not change.

Young and her co-workers have extensively used this method to derive rotational temperature from the CO_2 7820 and 8689 Å bands. In their latest paper (Schron *et al.* 1979) a value of $230 \pm 1K$ has been derived from the 8689 Å band. The value of b was found from (ii) to be more than 0.5 (but less than 1) indicating that the lines lie in the transition part of the curve-of-growth. This implies that the iteration procedure should be used. An average value for b of 0.67 for the 7820 Å CO_2 and 0.56 for the stronger 8689 Å band, was found. For Jupiter a rotational temperature of 184 ± 13 K has been derived by Margolis & Fox (1969a) based on the reflecting layer model.

(d) *Abundances* : It is also possible to compute the apparent amount of CO_2 in the absorption path from either (i) or (ii) above, (see Schorn *et al.* 1969, Young *et al.* 1975). It is evident that to use these methods it is necessary that the band be analysed and quantum numbers assigned. This has been done for the 7880 and 8669 Å bands of CO_2 in the spectrum of Venus. The analysis of Young (1972) shows an interesting trend (see her Table III), the derived abundance of the CO_2 decreases as we go from the red region to the infrared region. The abundance derived from the 2.2μ band is 6.6 times smaller than that derived from the 7820 Å band.

For Jupiter, Martin (1975) has derived an abundance of 25 cm-atm of NH_3 from the 1.96μ band, which after making an allowance for the uncertainty in the pressure broadening is 30 times smaller than that estimated from the 6450 Å band. For Jupiter only the R-branch of the $3\nu_3$ CH_4 band at 1.1μ has been theoretically analysed (Margolis & Fox 1969b, Bergstralah 1973). The other higher overtone bands in the visible region have not been analysed. For ammonia, which has a rich dipole spectrum like that of CH_4, vibrational quantum numbers have been assigned to 42 bands (McBride & Nicholls 1972a). The rotational analysis has also been carried out for the $5\nu_1$ band at 6441 Å (McBride & Nicholls 1972b), but because of the complexity of the band still much remains to be done. Ammonia abundances have been derived by Mason (1970) for the $5\nu_1$ and $4\nu_1$ (10800 Å) bands from comparison of the equivalent widths of lines in the bands in the Jovian spectrum with those obtained in the laboratory (see also the analysis of Young & Margolis 1977, Giver *et al.* 1975). Smith *et al.* (1980) have used an inhomogeneous

model and derived an abundance of 1.5 m-atm. In contrast, Mason had derived an abundance of 13 m-atm, Young & Margolis 16.4 m-atm and Giver *et al.* 10 m-atm.

It is common to derive abundances using atmospheric models. The abundances are varied so that the computed lines profiles match the observed (Regas *et al.* 1975) ones. Teifel (1977b), using a similar approach based on a scattering model, arrived at an abundance of 0.31 m-amagat for ammonia. For CH_4 an abundance of 10-20 m-amagat is derived. Earlier, for CH_4 Bergstralah (1973) had found an abundance of about 50 m-amagat on the basis of a reflecting layer model.

(e) *Polarization* : Much more information can be obtained from the study of the polarization along the line (Buriez *et al.* 1979) : (i) cloud top heights, (ii) scale height ratios of the gas-to-cloud particles and gas-to-gas, and (iii) the verticle profile of the atmosphere. Hunt (1973b) also uses the equivalent widths to find vertical structure of Jupiter's atmosphere. Sobolev (1972) gives profiles and equivalent widths which can be used to deduce the vertical distribution of aerosols and molecules. Michalsky *et al.* (1974) have used the molecular band variations as probe of the vertical structure of Jupiter's atmosphere.

Polarization (other than in the line) is a potentially powerful tool to deduce the nature of particles. Hansen & Hovenier (1974) have been able to reproduce the phase variation of the polarization of Venus using a combination of Mie and Rayleigh scattering. Morzhenko & Yanovitskii (1973) have used polarization studies to obtain the properties of Jupiter and Venus clouds.

(f) *Other techniques :* Limb-darkening scans, the variation of brightness over the disks of Jupiter and Venus and the variation of intensity with wavelength are the other probes (Pilcher & McCord 1971, Pilcher *et al.* 1973, Pilcher & Kunkle, 1976, Munch & Younkin 1974, Axel 1972, Teifel 1976, Dlugach & Yanovitskii 1974, Orton 1975; Dollfus *et al.* 1975, Diner & Westphal 1977; West 1979a, b; Herman *et al.* 1979) which have been used to obtain cloud parameters.

8. Future needs

While concluding this review we give below some research problems which need urgent attention.

(a) *Theoretical work*

(i) Because of the difficult nature of the problem, very few analytial studies have been made of inhomogeneous atmospheres in which the albedo changes with the optical depth (Abhyankar & Fymat 1970*a,b,c*; Fymat & Abhyankar 1969*a,b*; Sobolev 1963, 1975; Ueno 1960; Busbridge 1961). Based on the work of Abhyankar & Fymat tables need to be computed to calculate the intensity of reflected radiation from such an atmosphere.

(ii) On the basis of thermodynamical arguments, Lewis (1969) showed that a multi-layered atmospheric model is more realistic. Later studies and the space fly-bys strengthen the argument for such a model. Theory of such models is still to be worked out.

(iii) The topmost layer will invariably involve gaseous scattering represented by Rayleigh's phase matrix. Although we have tables for non-conservative Rayleigh scattering for a semi-infinite atmosphere (Abhyankar & Fymat *op. cit.*, Lenoble *op. cit.*), none exist for a finite atmosphere. Sekera's (1966a, b) work can be used to compute these tables. Alternatively, the doubling method can be used.

(iv) The bands of NH_3 and CH_4 have to be quantum analysed.

(b) *Observational work*

(i) Observations with high time and space resolutions are badly needed to decide between different models.

(ii) Only recently Wolstencroft & Smith (1979) have attempted to measure polarisation along the band at a resolution of 10 Å. Clearly, higher dispersion observations are needed. With modern detectors it should be possible to obtain spectra with a polaroid in different orientations in front of the slit of the spectrograph. Fourier transform spectroscopy can also be used (Fymat & Abhyankar 1970).

(iii) While vertical inhomogenity has received a lot of attention only one study of horizontal inhomogenity has been made (Appelby & Blerkom 1975). Observations by Cochran & Cochran (1980) show that the atmosphere of Jupiter shows longitudinal variations in the equivalent widths. This is another area where more work is required.

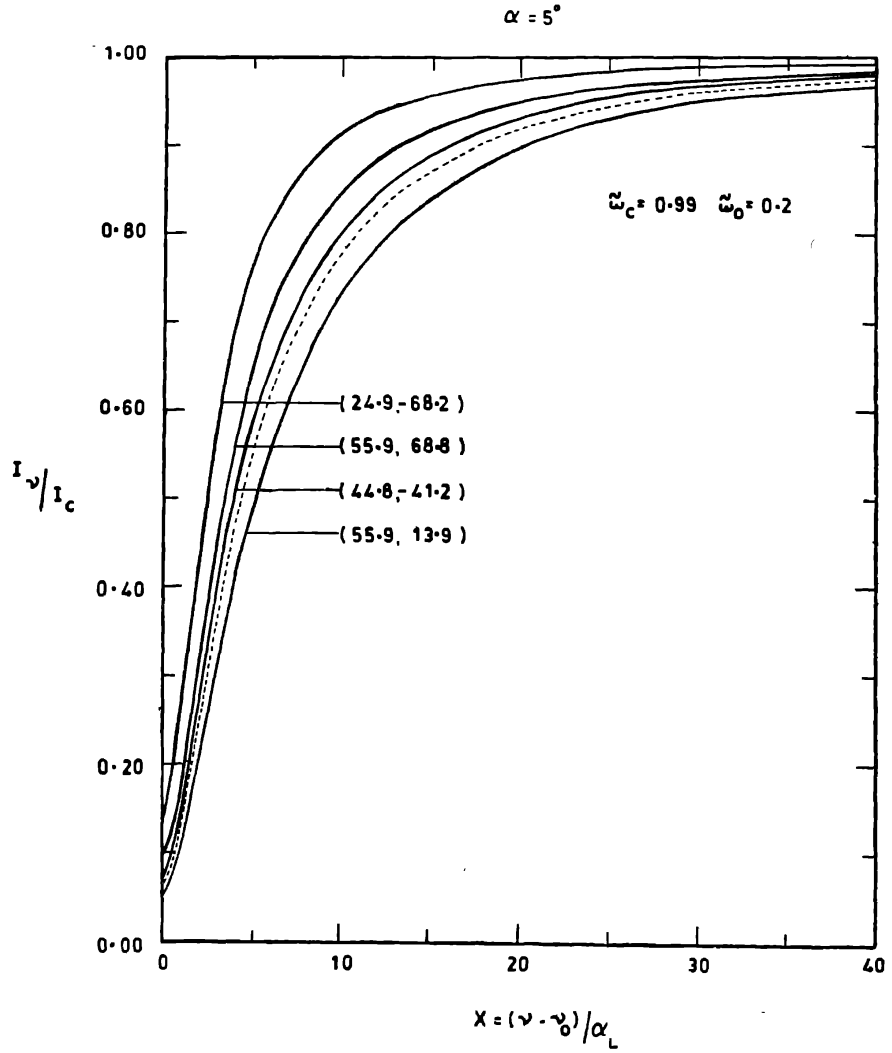

(Read colatitude 77.1 for 55.9, 51.4 for 44.8 and 25.7 for 24.9)

Figure 4. The abscription line profiles for phase angle 5° in the integrated light (dashed line) and for four points on the disk (solid lines) whose co-latitude and longitude are given in brackets, for $\tilde{\omega}_0 = 0.2$.

(iv) As mentioned earlier, Hansen and Hovenier explained the polarization phase curve of Venus on the basis of an atmosphere in which Mie-scattering is dominant. Based on such a model, they computed the visual phase curve. An interesting feature of the computed phase-curve is a dip at a phase angle of about 10° (see van de Hulst 1980, Hansen & Travis 1974—Figure 32). This needs to be checked against observations, which is very difficult because of the contamination due to scattering of sunlight by earth's atmosphere.

(v) An additional constraint on the models is the equivalent-width phase-curve of Venus. As in (iv) above if a Mie-scattering model is used a dip at a phase angle of about 10° is required. Young *et al.* (1980) have presented observations from 1967 and 1975 for the 7820-, 7883- and 8689-Å CO_2 bands. Of these, the 8689-Å band, which is the strongest, shows no dip, while there seems to be a dip in the weaker 7820- and 7883-Å bands. One reason for this discrepancy could be the day-to-day

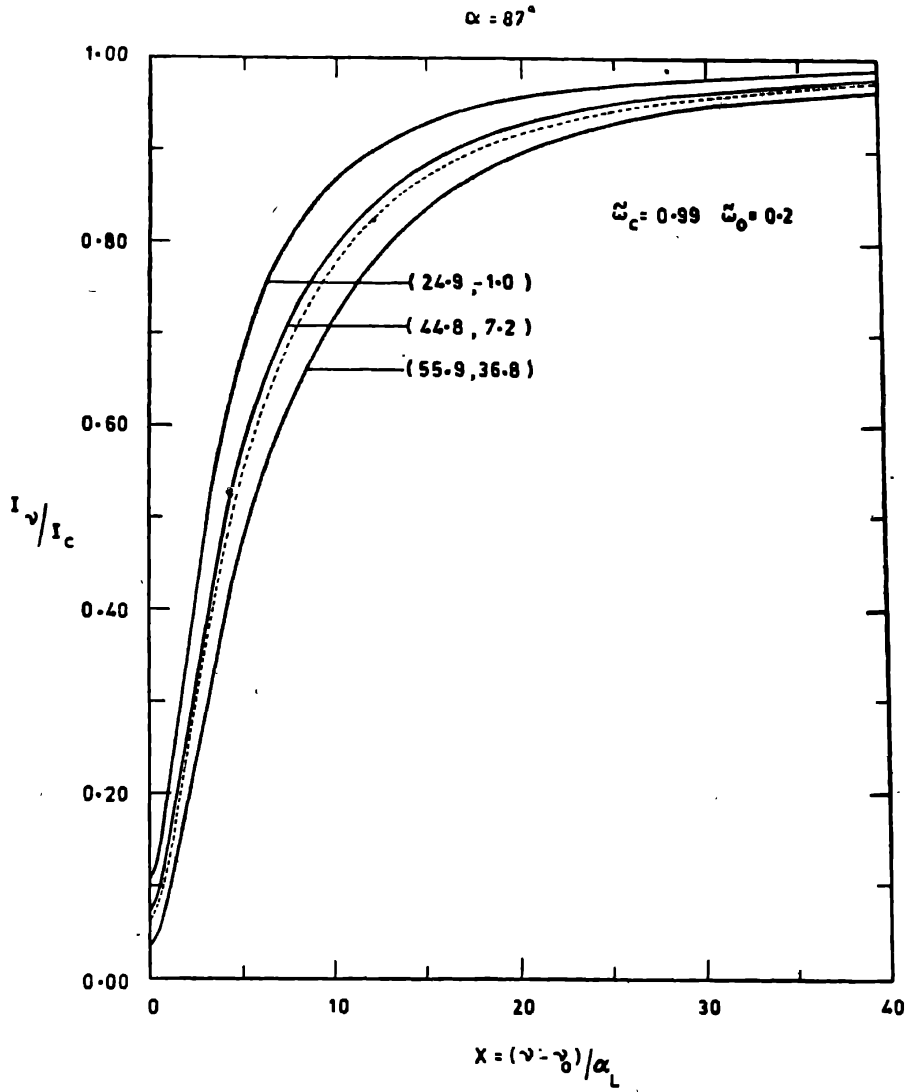

(Read colatitude 77.1 for 55.9, 51.4 for 44.8 and 25·7 for 24.9)

Figure 5. Same as in Figure 4 but for phase angle 87°. The line profile at (1.77, 74.7) is very close to the profile in the integrated light and is not shown separately.

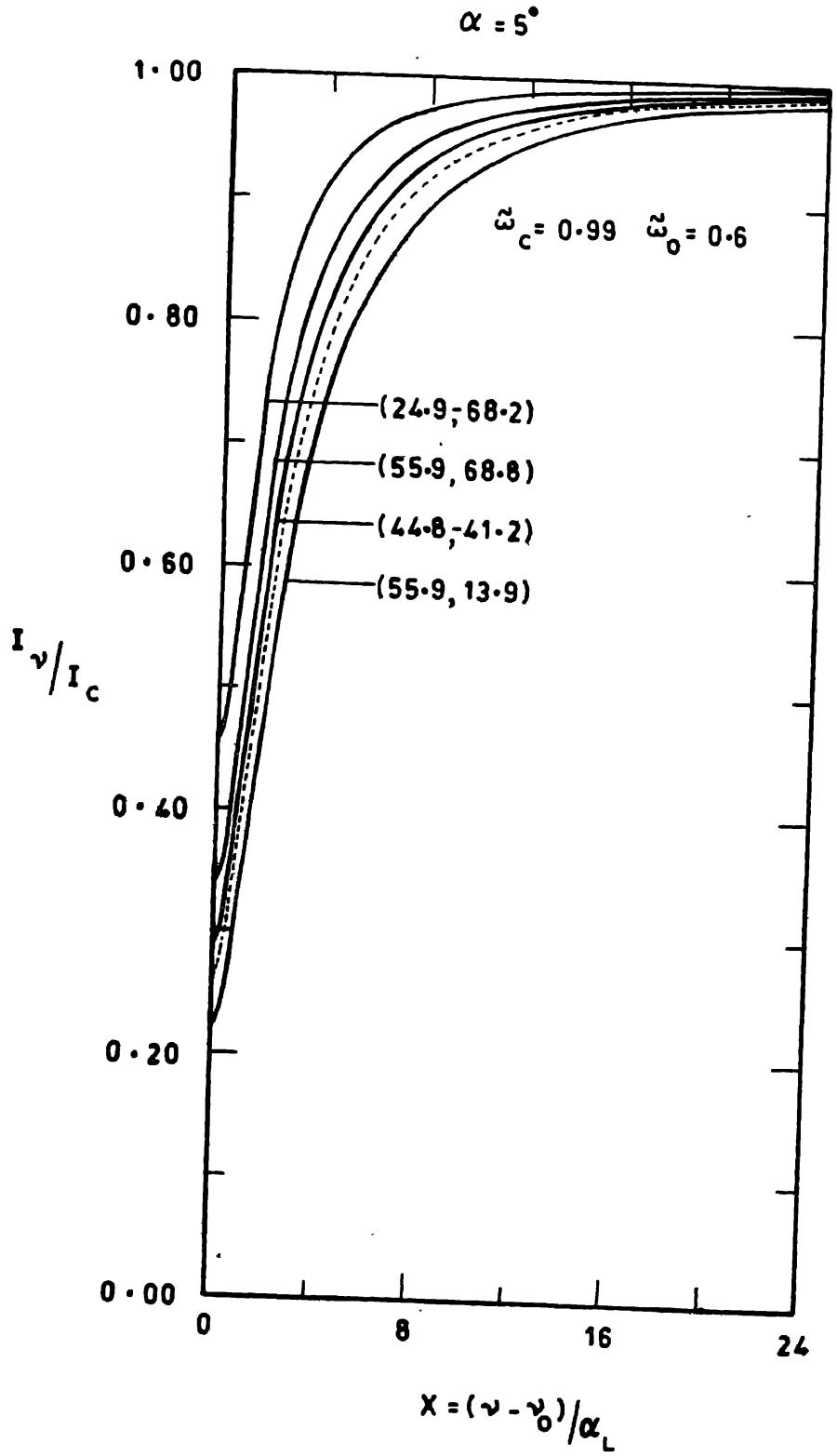

(Read colatitude 77.1 for 55.9, 51.4 for 44.8 and 25.7 for 24.9)

Figure 6. Same as in Figure 4, but for $\tilde{\omega}_0 = 0.6$.

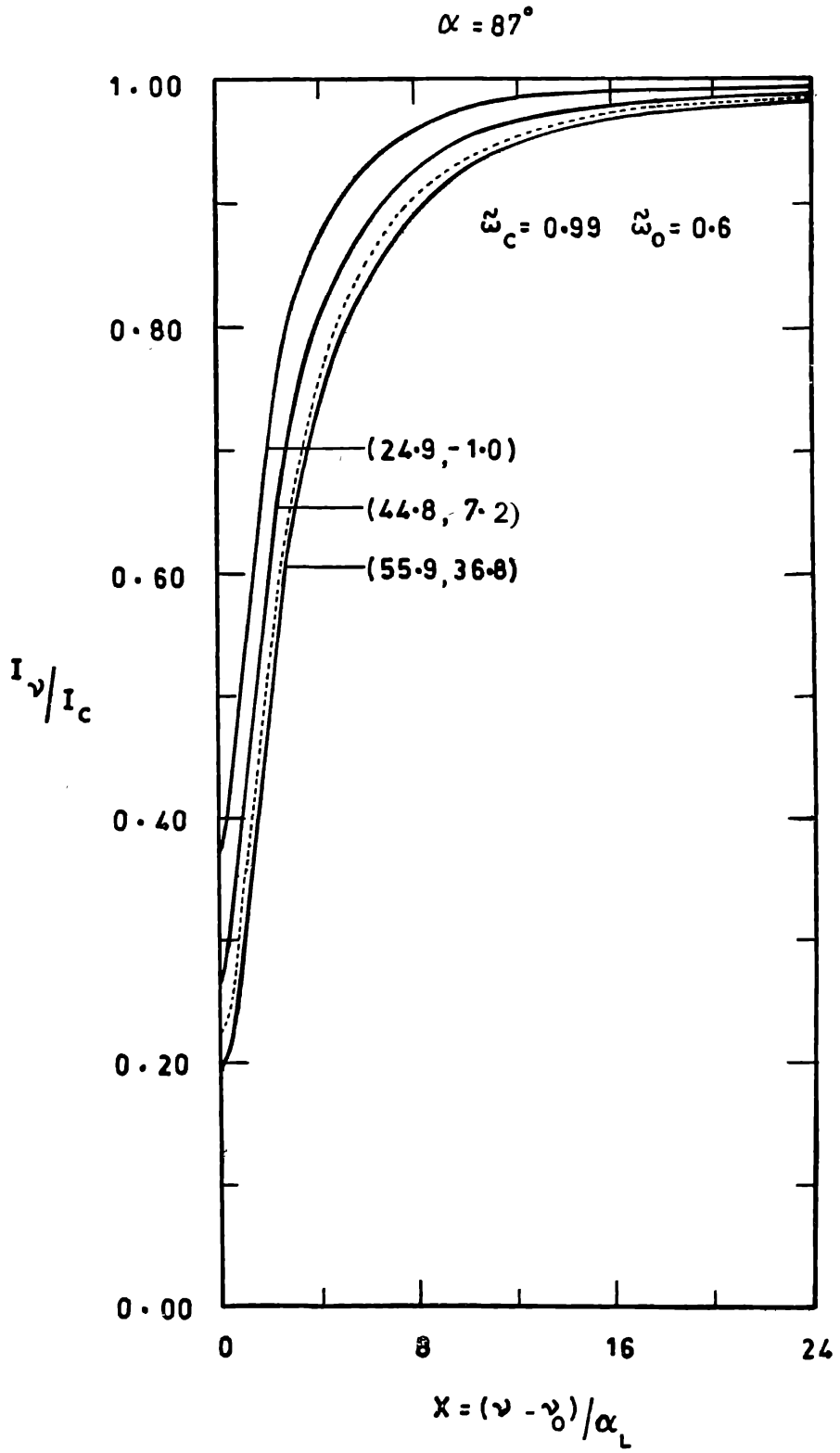

(Read colatitude 77.1 for 55.9, 51.4 for 44.8 and 25.7 for 24.9)

Figure 7. Same as in Figure 5, but for $\tilde{\omega}_0 = 0.6$.

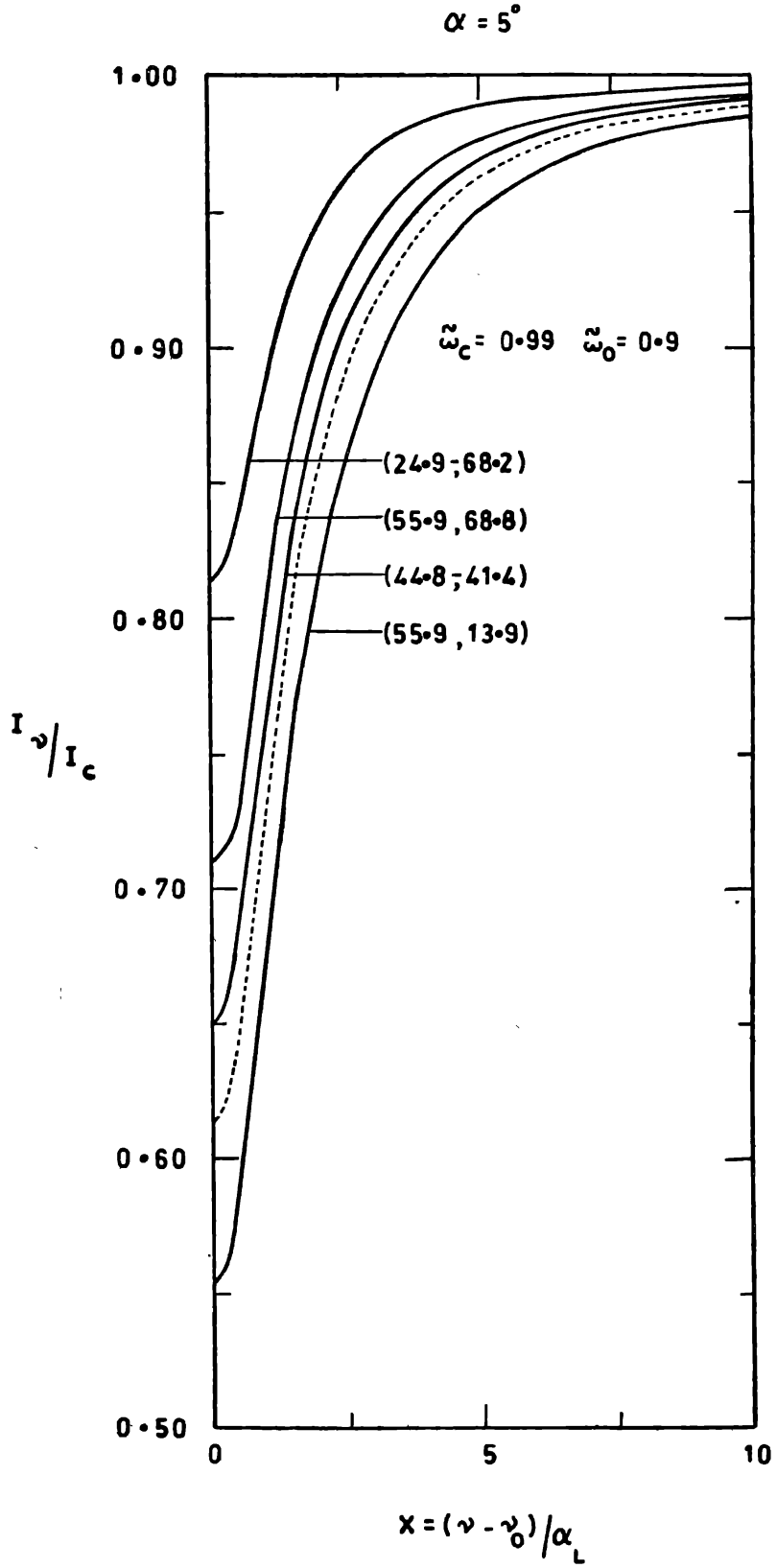

(Read colatitude 77.1 for 55.9, 51.4 for 44.8 and 25.7 for 24.9)

Figure 8. Same as in Figure 4, but for $\tilde{\omega}_0 = 0.9$.

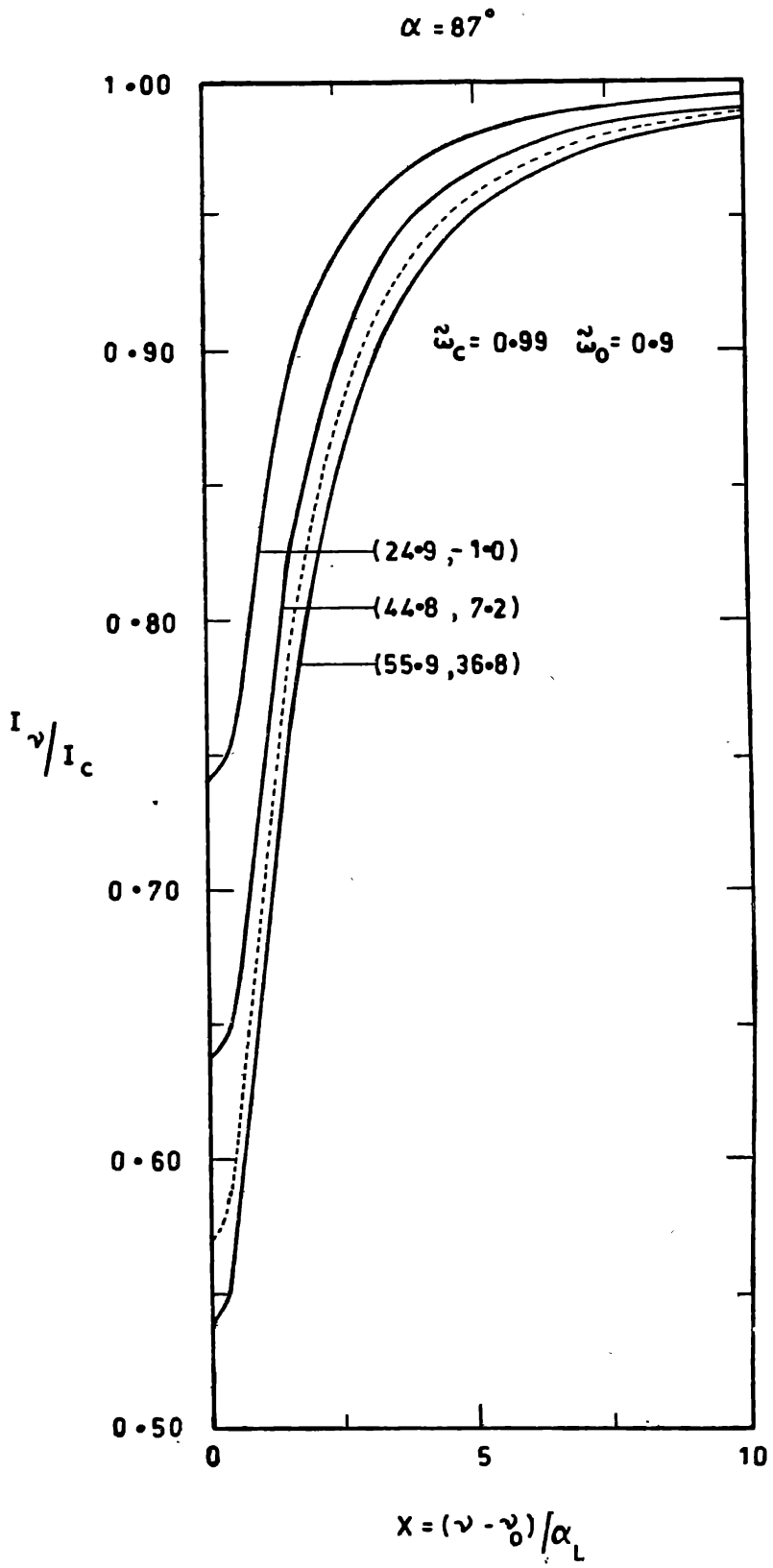

(Read colatitude 77.1 for 55.9, 51.4 for 44.8 and 25.7 for 24.9)

Figure 9. Same as in Figure 5, but for $\tilde{\omega}_0 = 0.9$.

fluctuations of the concentration of CO_2 in the Venus atmosphere. Simultaneous observations of these bands are required to see whether this is the case.

9. Our approach to the problem

Assuming a semi-infinite Rayleigh scattering atmosphere, we have computed absorption and polarization line profiles using the Rayleigh phase matrix, *i.e.*, taking polarization into account in computing the intensity (*cf.* equations 27, 29, 38, 39, 40 and 45). This is important because Rayleigh's phase function gives only qualitative results, for a complete picture polarization has to be taken into account. Components of the intensity vector were calculated by using Lenoble's (1970) tables. Quite often, as mentioned earlier, only the integrated light from the whole disk is observed. We have therefore, used Horak's (1950) method for such integration. We are presenting here results for the absorption and polarization line profiles for four points on the disk, and also absorption line profiles in the integrated light from the whole disk, for two phase angles, 5° and 87°. Lines of three different intensities have been chosen: (i) albedo at line centre 0.2, (ii) albedo at line centre 0.6, (iii) albedo at line centre 0.9. A continuum albedo of 0.99 has been assumed in all cases.

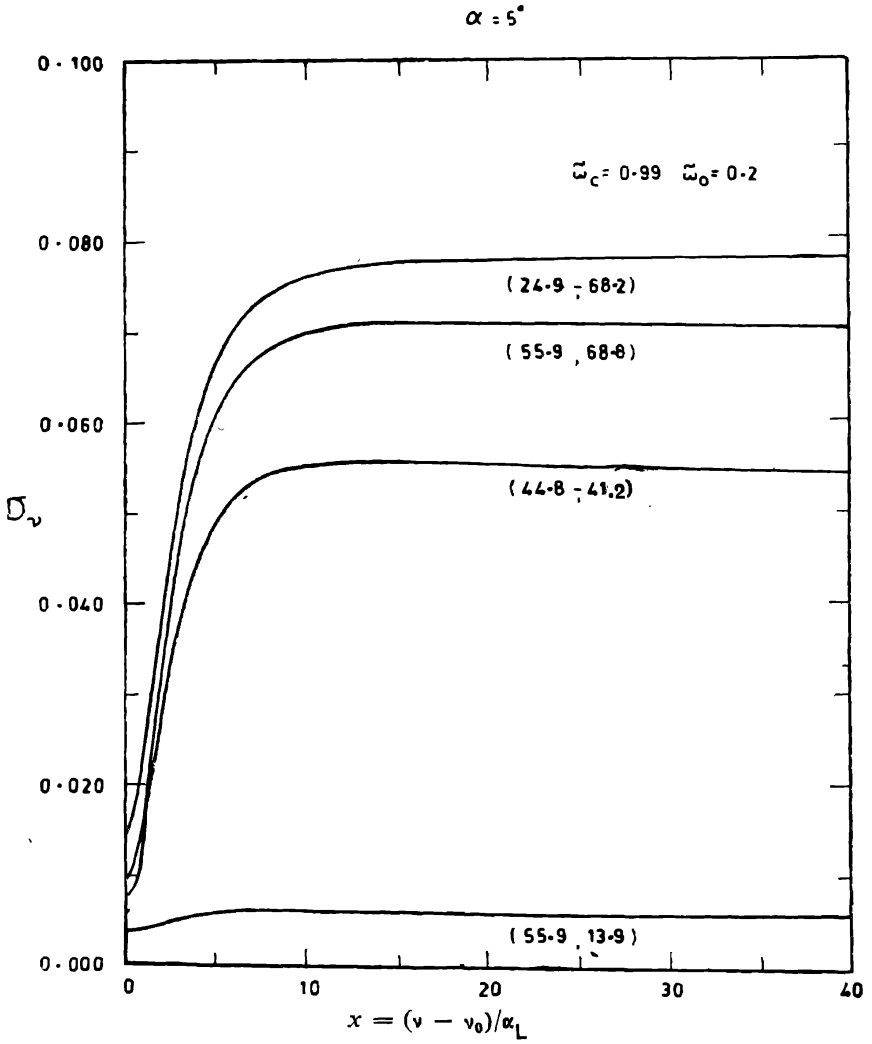

(Read colatitude 77.1 for 55.9, 51.4 for 44.8 and 25.7 for 24.9)

Figure 10. Polarization line profiles for phase angle 5° ($\tilde{\omega}_0 = 0.2$) (see legend for Figure 4).

(a) *The absorption line profiles* : These are shown for the three cases (i) in Figures 4 and 5, (ii) in Figures 6 and 7 and (iii) in Figures 8 and 9. The dashed line shows the profile in the integrated light of the disk and the solid lines for different points on the disk. The numbers in parantheses are the co-latitude and the longitude measured from the sub-earth point. These are representative points from the grid shown in Figure 3 which is set up on the disk to perform the integration. For the phase angle 5°, the line at the point with coordinates (77.1, 13.9) is the strongest and that at (25.7, −68.2) the weakest. Comparison of lines at (77.1, 13.9) and (77.1, 68.8) shows that for the same co-latitude, there is a weakening of lines as we go towards the limb—a fact which is in accord with observations. A similar trend is seen for phase angle 87°, where the line at (77.1, 13.9) is stronger than the line at (77.1, 74.7) which is not shown separately because it is close to the dashed line for the total flux. Again for 5°, if a comparison is made between the lines at (51.4, −41.2) and (25.7, −68.2), a weakening of absorption will be noticed towards the poles. This can also be seen for phase angle 87° on comparing line profiles at (51.4, 7.2) and (25.7, −1.0).

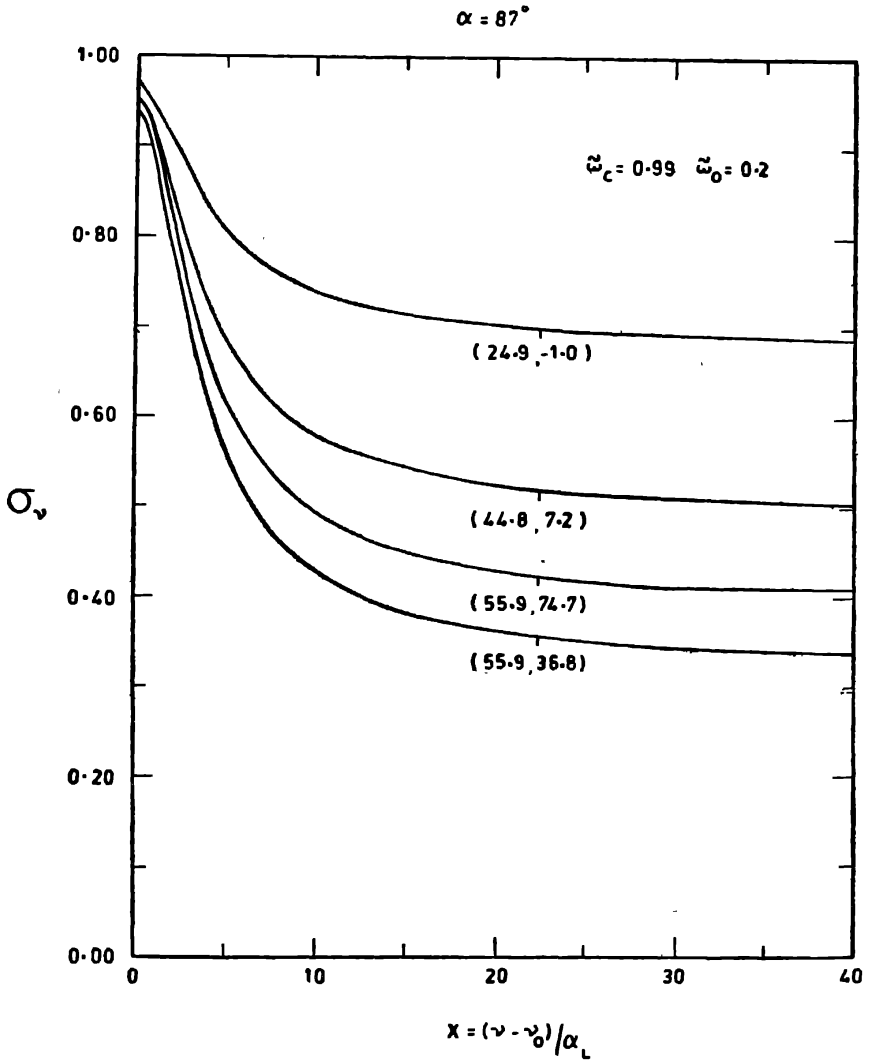

(Read colatitude 77.1 for 55.9, 51.4 for 44.8 and 25.7 for 24.9)

Figure 11. Polarization line profiles for phase angle 87° ($\tilde{\omega}_0 = 0.2$) (see legend for Figure 5).

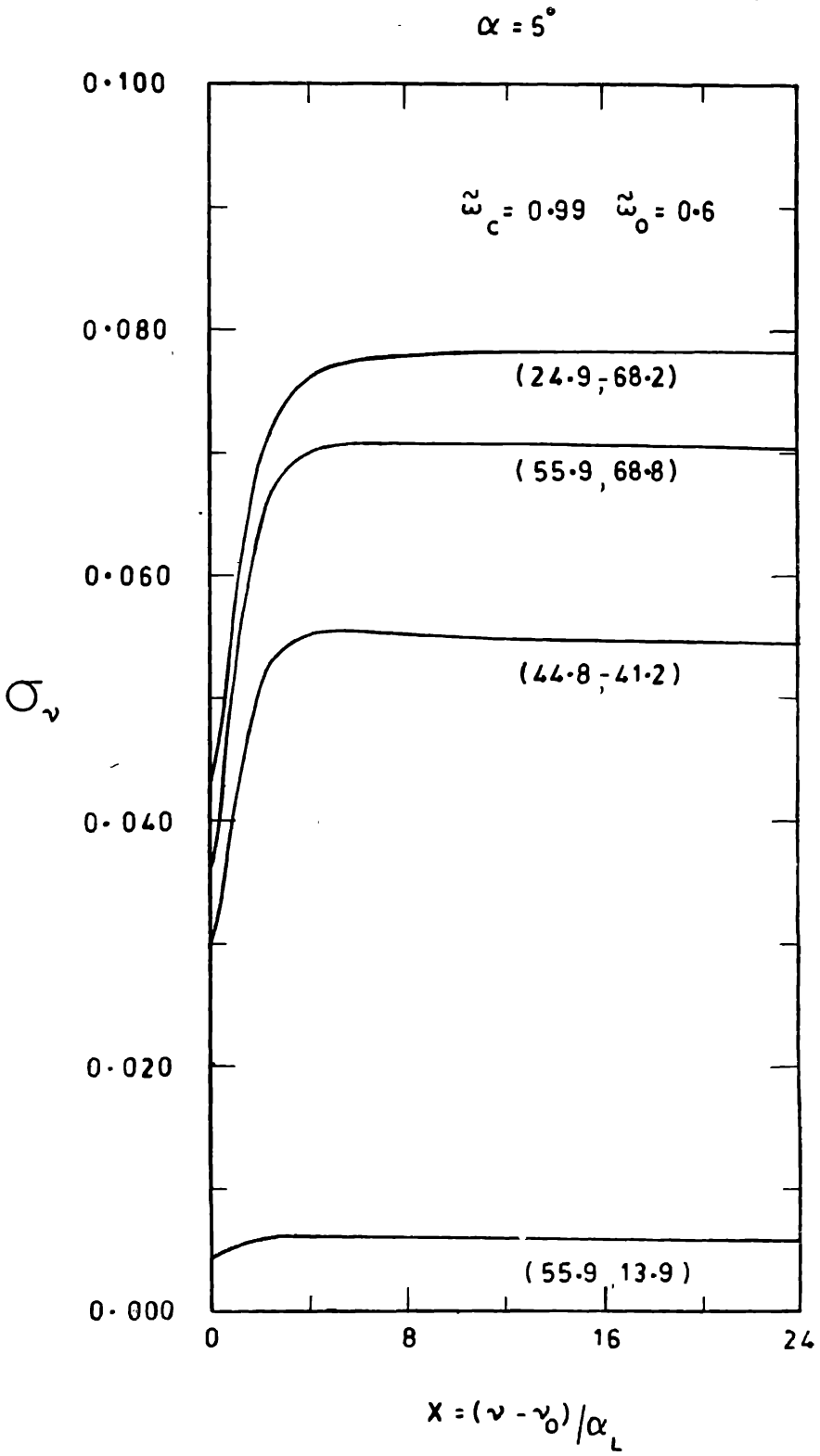

(Read colatitude 77.1 for 55.9, 51.4 for 44.8 and 25.7 for 24.9)

Figure 12. Same as in Figure 10 but for $\tilde{\omega}_0 = 0.6$.

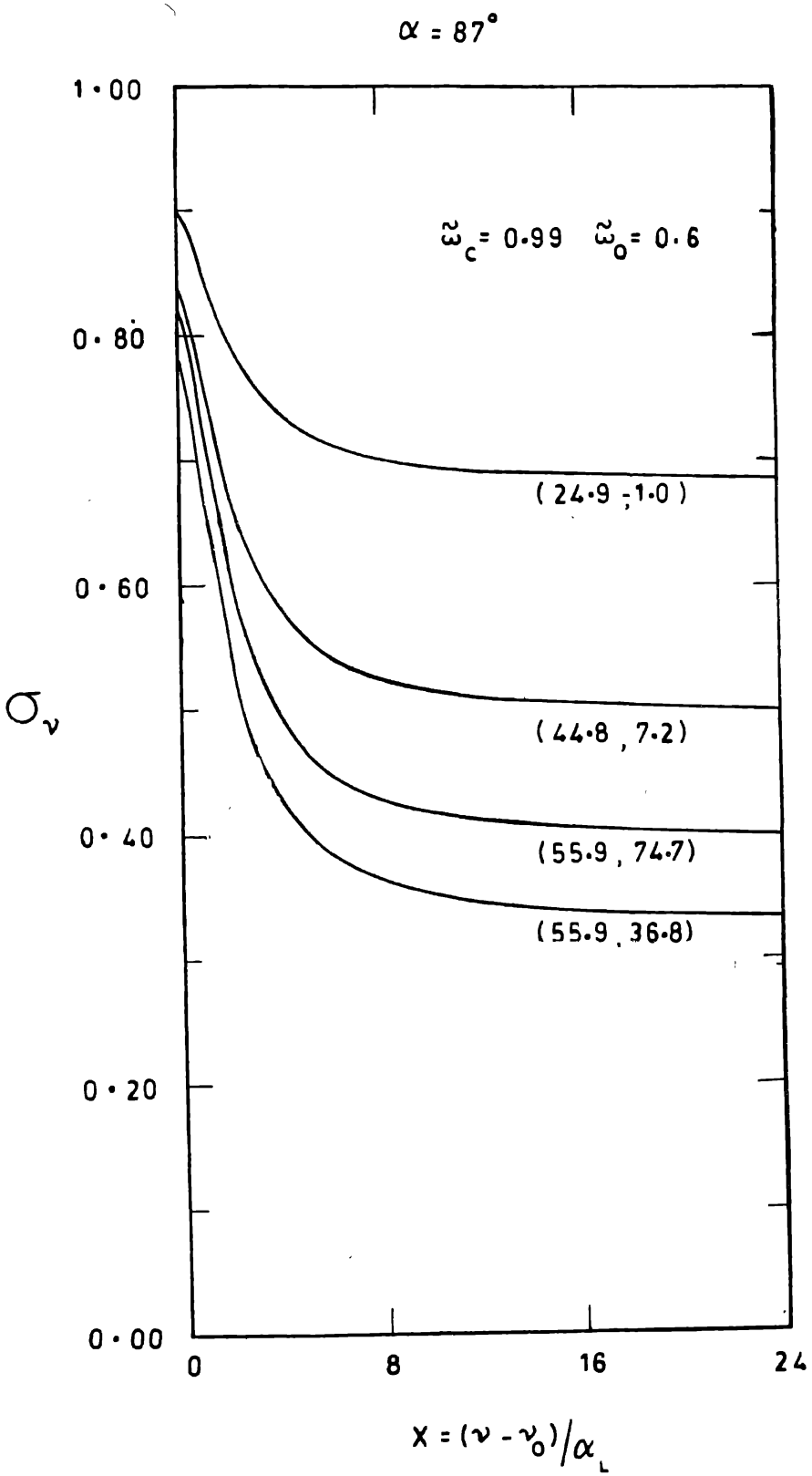

(Read colatitude 77.1 for 55.9, 51.4 for 44.8 and 25.7 for 24.9).

Figure 13. Same as in Figure 11 but for $\tilde{\omega}_0 = 0.6$.

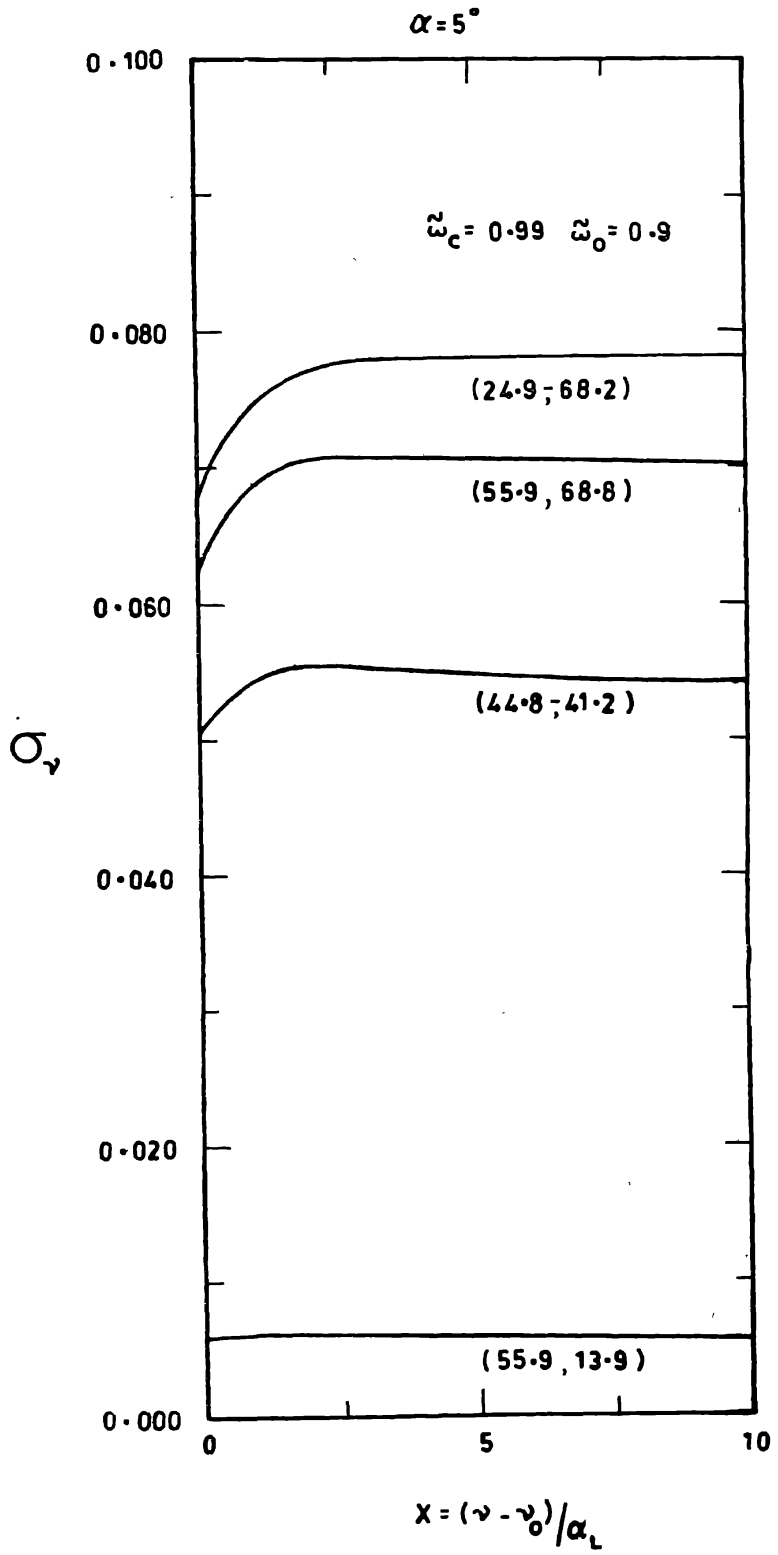

(Read colatitude 77.1 for 55.9, 51.4 for 44.8 and 25.7 for 24.9)

Figure 14. Same as in Figure 10 but for $\tilde{\omega}_0 = 0.9$.

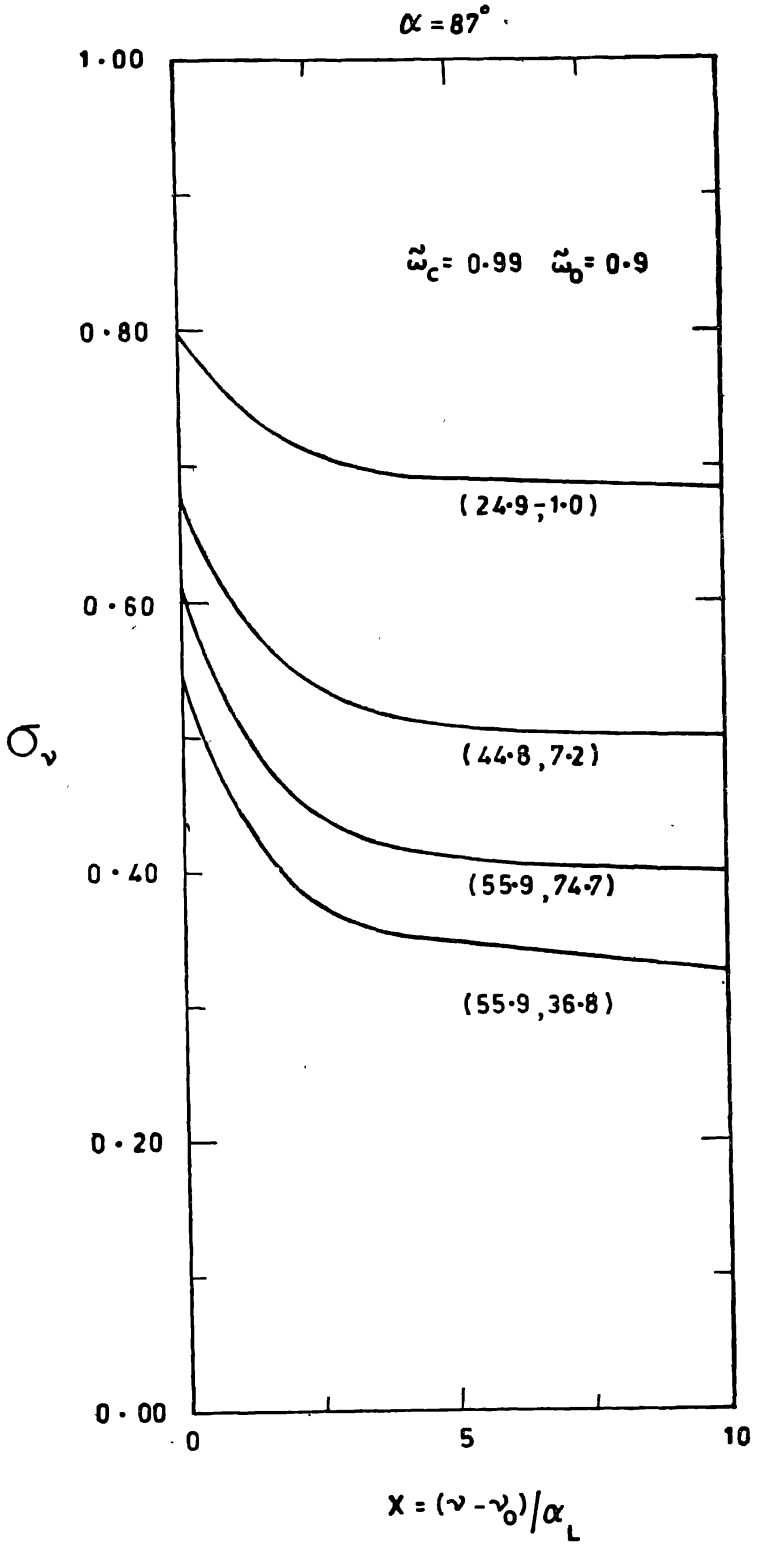

(Read colatitude 77.1 for 55.9, 51.4 for 44.8 and 25.7 for 24.9)

Figure 15. Same as in Figure 11 but for $\tilde{\omega}_0 = 0.9$.

(b) *The polarization line profiles*: These are shown for the three cases mentioned earlier : (i) in Figures 10 and 11, (ii) in Figures 12 and 13 and (iii) in Figures 14 and 15. In this case there is a distinct difference for the two phase angles. For 87° the polarization is maximum at line centre and decreases towards the wings, a fact which is attributed to multiple scattering. At the centre of the line, because of more absorption relative to the wings, the observed radiation would have undergone fewer number of scatterings compared to the radiation in the wings. Therefore, the depolarization effect in the wings would reduce the degree of polarization. However at 5° just the opposite is seen : the degree of polarization increases towards the wings. It should be noted that at 87° the polarization at line centre is high while at 5° it is low. It might be possible that when the polarization carried by the initial orders of scattering is low multiple scattering might actually increase the polarization; this can be checked using the Monte-Carlo method.

The variation of polarization over the disk brings out the fact that it is inaccurate to use equation (30) to compute the polarization. For a particular phase angle the

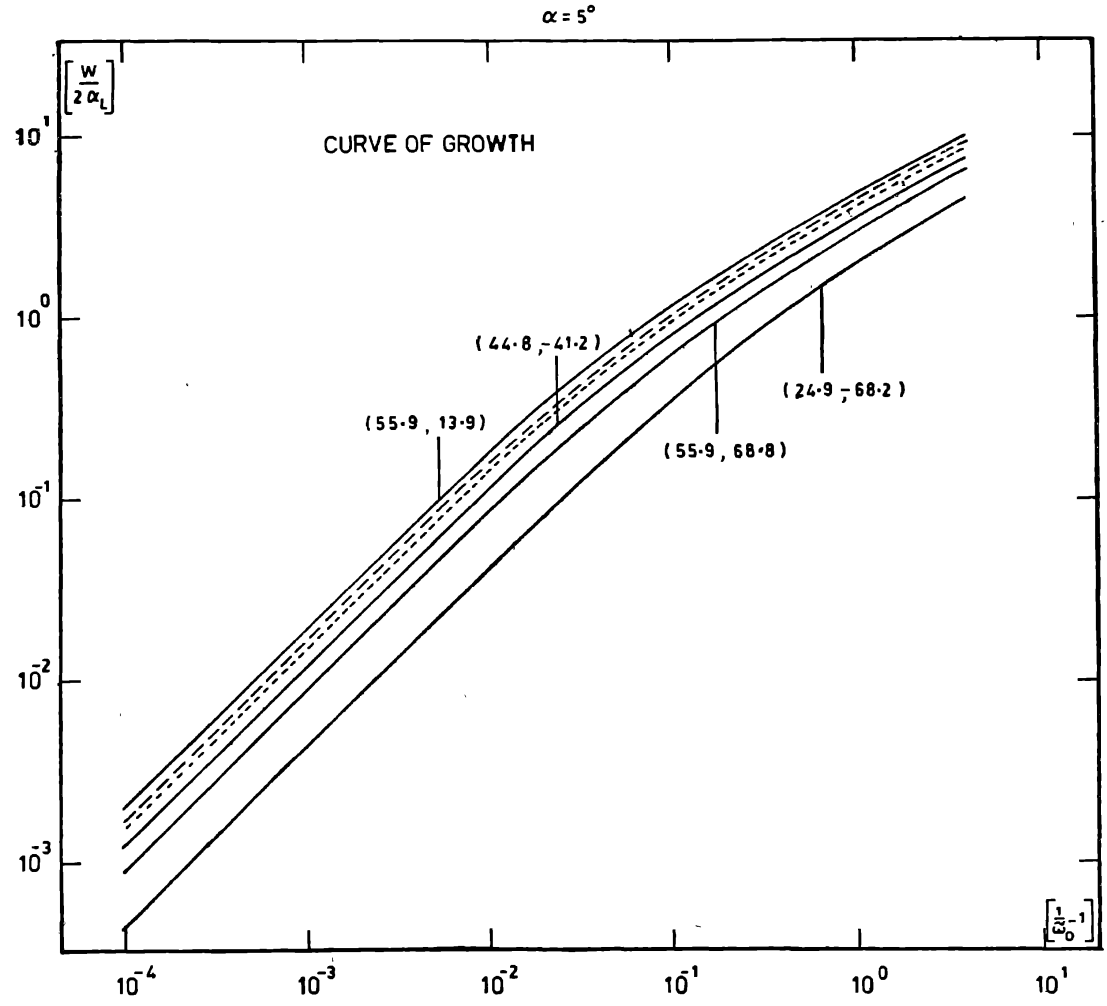

(Read colatitude 77.1 for 55.9, 51.4 for 44.8 and 25.7 for 24.9)

Figure 16. The curves-of-growth for phase angle 5° (see legend for Figure 4). The abscissa is $(\tilde{\omega}_0^{-1} - 1)$ which is proportional to the line intensity. The curve for 87° in integrated light is shown by long dashes, for comparison.

plane of scattering is fixed and the variation over the disk is due to the different inclinations of the meridian planes—defining the directions of the sun and the earth to that of the scattering plane (*cf.* Chandrasekhar 1960, p. 38). Therefore one must use equation (29) and not (30). It also brings into focus the inadequacy of Rayleigh phase function.

(*c*) *Curve-of-growth* : It gives the variation of equivalent width as a function of line intensity. Figures 16 and 17 show these curves for the two phase angles. The two regimes *viz.* the linear and the square-root part are clearly separated by a transition region. For different points on the disk, the curves are simply shifted along the ordinate, depending on the strength of absorption. Comparison of the curves in the integrated light for the two phase angles brings out the fact the absorption at 87° is stronger than at 5°. This, as mentioned earlier, is in accordance with observations.

The work is continuing and detailed results for complete phase variation of the intensity and polarization profiles and the curves-of-growth will be reported in another paper.

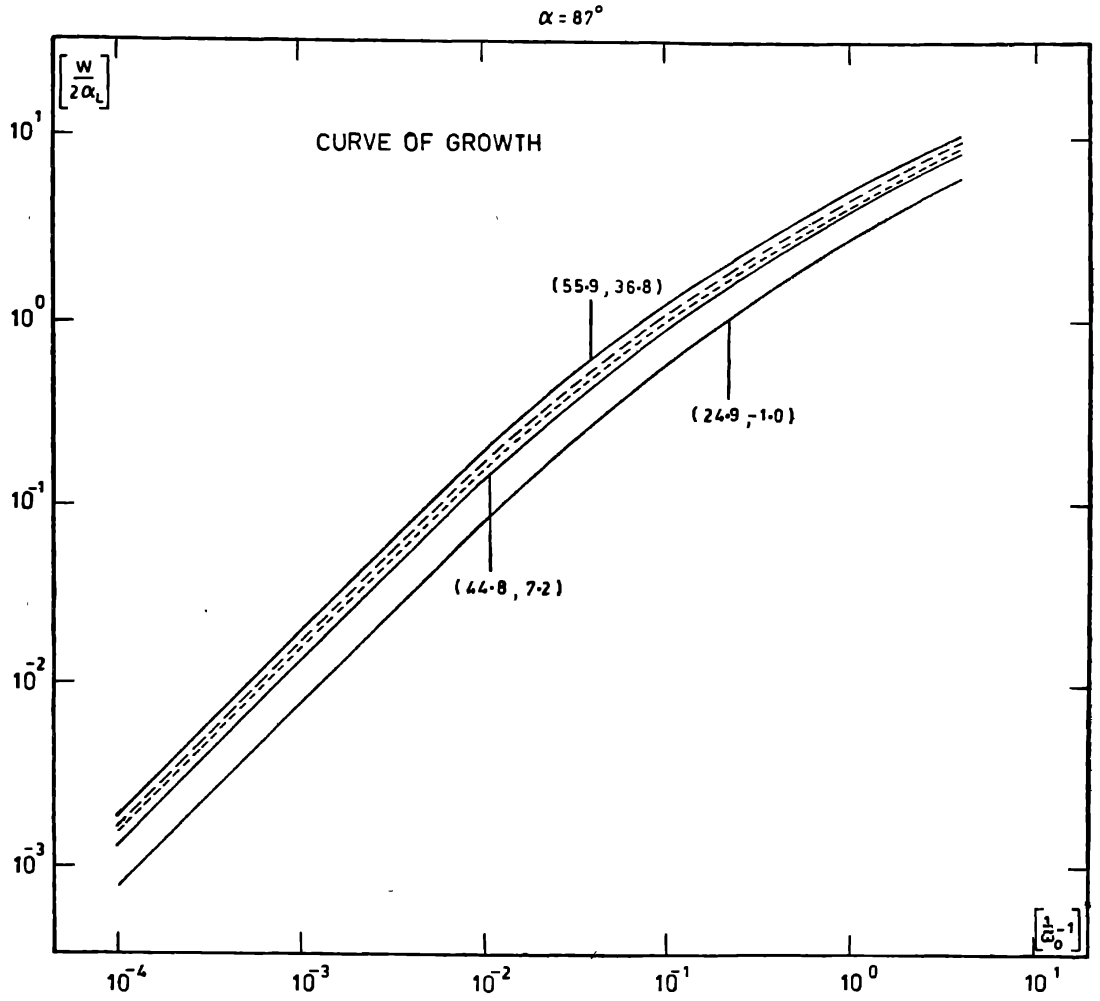

Figure 17. The curves-of-growth for phase angle 87° (see legend for Figure 5). Short dashes show the curve for 5° in integrated light.

Acknowledgements

R.K.B. would like to thank the University Grants Commission, New Delhi, for the award of a Research Fellowship.

References

Abhyankar, K. D. & Fymat, A. L. (1970a) *Ap. J.* **159**, 1009.
Abhyankar, K. D. & Fymat, A. L. (1970b) *Ap. J.* **159**, 1019.
Abhyankar, K. D. & Fymat, A. L. (1970c) *Astr. Ap.* **4**, 101.
Adams, W. S. & Dunham, T. (1932) *Publ. astr. Soc. Pacific* **44**, 243.
Adel, A. (1937) *Ap. J.* **86**, 337.
Anikonov, A. S. (1977) *Sov. Astr.* **21**, 95.
Appelby, J. F. & van Blerkom, D. J. (1975) *Icarus* **24**, 51.
Avery, R. W., Michalsky, J. J., & Stokes, R. A. (1974) *Icarus* **21**, 47.
Avramchuk, V. V. (1970) *Sov. Astr.* **14**, 462.
Axel, L. (1972) *Ap. J.* **173**, 451.
Barker, E. S. & Perry, M. A. (1975) *Icarus* **25**, 282.
Barker, E. S. & Macy Jr, N. M. (1977) *Icarus* **30**, 551.
Baum, W. A. & Code, A. D. (1953) *Astr. J.* **58**, 108.
Beer, R. & Taylor, F. W. (1973) *Ap. J.* **179**, 309.
Belton, M. J. S. (1968) *J. Atmos. Sci.* **25**, 596.
Belton, M. J. S., Hunten, D. M. & Goody, R. M. (1968) in *The Atmospheres of Venus and Mars*, Gordon and Breach.
Bergstralah, J. T. (1973) *Icarus* **19**, 390.
Binder, A. B. (1972) *Astr. J.* **77**, 93.
Binder, A. B. & McCarthy, D. W. (1973) *Astr. J.* **78**, 939.
Boese, R. W., Miller, J. H. & Inn, E. C. Y. (1966) *J. Quant. Spectrosc. Radiat. Transfer* **6**, 717.
Boyce, P. B. (1968) *Lowell Obs. Bull.* **146**, 93.
Buriez, J. C., Fouquart, Y. & Fymat, A. L. (1979) *Astr. Ap.* **79**, 287.
Busbridge, I. W. (1961) *Ap. J.* **133**, 198.
Carleton, N. P. & Traub, W. A. (1974) in *Exploration of the Planetary System* (eds : A. Woszczyk & C. Iwanizewska) D. Reidel, p. 345.
Chamberlain, J. W. & Kuiper G. P. (1956) *Ap. J.* **124**, 399.
Chamberlain, J. W. (1965) *Ap. J.* **141**, 1184.
Chamberlain, J. W. (1970) *Ap. J.* **144**, 1148.
Chamberlain, J. W. & Smith, G. (1970) *Ap. J.* **160**, 755.
Chandrasekhar, S. (1960) *Radiative Transfer*, Dover.
Cochran, W. D. (1977) *Icarus* **31**, 325.
Cochran, W. D. & Cochran, A. L. (1980) *Icarus* **42**, 102.
Danielson, R. E. & Tomasko, M. G. (1969) *J. Atmos. Sci.* **26**, 889.
Dicke, R. H. (1953) *Phys. Rev.* **89**, 472.
Diner, D. & Westphal, J. (1977) *Icarus* **32**, 299.
Dlugach, J. M. & Yonovitskii, E. G. (1974) *Icarus* **22**, 66.
Dollfus, A. *et al.* (1975) *Icarus* **26**, 53.
Dunham, T. (1949) in *The Atmospheres of the Earth and Planets* (ed : G. P. Kuiper) University of Chicago Press.
Fountain, J. W. (1972) *Comm. Lunar Planet. Lab.* **9**, 327.
Fymat, A. L. (1974) in *Planets Stars and Nebulae* (ed : T. Gehrels) University of Arizona Press, Tuscon.
Fymat, A. L. & Abhyankar, K. D. (1969a) *Ap. J.* **158**, 315.
Fymat, A. L. & Abhyankar, K. D. (1969b) *Ap. J.* **158**, 325.
Fymat, A. L. & Abhyankar, K. D. (1970) *Appl. Optics* **9**, 1075.
Giver, L. P., Miller, J. H. & Boese, R. W. (1975) *Icarus* **25**, 34.
Goody, R. M. (1964) in *Atmospheric Radiation I*, Oxford University Press.

Gray, L. D. (1969) *Icarus* **10**, 90.
Hansen, J. E. & Hovenier J, W. (1974) *J. Atmos. Sci.* **31**, 1137.
Hansen, J. E. & Travis, L. D. (1974) *Space Sci. Rev.* **16**, 527.
Herman, M., Devaux, C. & Dollfus, A. (1979) *Icarus* **37**, 282.
Herzberg G. (1951) *J. Roy. Astr. Soc. Canada* **45**, 100.
Hess, S. L. (1953) *Ap. J.* **118**, 151.
Horak, H. G. (1950) *Ap. J.* **112**, 445.
Hunt, G. E. (1972a) *J. Quant. Spectrosc. Radiat. Transfer* **12**, 387.
Hunt, G. E. (1972b) *J. Quant. Spectrosc. Radiat. Transfer* **12**, 405.
Hunt, G. E. (1973a) *J. Quant. Spectrosc. Radiat. Transfer* **13**, 465.
Hunt, G. E. (1973b) *Icarus* **13**, 637.
Hunt, G. E. (1973c) *M. N. R. A. S.* **161**, 347.
Hunt, G. E. & Bergstralh, J. T. (1974) *Nature* **249**, 635.
Hunt, G. E. & Berstralh, J. T. (1977) *Icarus* **30**, 511.
Irvine, W. M. (1975) *Icarus* **25**, 175.
James, T. C. (1969) *J. opt. Soc. Amer.* **59**, 1602.
Kattawar, G. W. & Young, L. D. G. (1977) *Icarus* **30**, 179.
Kiess, C. C., Corliss, C. H. and Kiess, A. K. (1960) *Ap. J.* **132**, 221.
Kuiper, G. P. (1952) in *The Atmospheres of the Earth and Planets* (ed : G. P. Kuiper) University of Chicago Press.
Kuiper, G. P. (1972) *Comm. Lunar Planet. Lab.* **9**, 249.
Lenoble, J. (1968) *J. Quant. Spectrosc. Radiat. Transfer* **8**, 641.
Lenoble, J. (1970) *J. Quant. Spectrosc. Radiat. Transfer* **10**, 533.
Lewis, J. S. (1969) *Icarus* **10**, 365.
Macy Jr, W. (1976) *Icarus* **29**, 49.
Macy Jr, W. & Trafton, L. (1977) *Icarus* **32**, 27.
Margolis, J. S. & Fox, K. (1969a) *Ap. J.* **157**, 935.
Margolis, J. S. & Fox, K. (1969b) *Ap. J.* **158**, 1183.
Martin T. Z. (1975) *Ph.D. Dissertation*, University of Hawaii.
Martin, T. Z., Cruikshank, D. R., Pilcher, C. B. & Sinton, W. M. (1976) *Icarus* **27**, **391**.
Mason, H. P. (1970) *Ap. Sp. Sci.* **7**, 424.
McBride, J. D. P. & Nicholls, R. W. (1972a) *J. Phys.* **B 5**, 408.
McBride, J. D. P. & Nicholls, R. W. (1972b) *Can. J. Phys.* **50**, 93.
McClatchey, R. A. (1967) *Ap. J.* **148**, 193.
McElroy, M. B. (1969) *J. Atmos Sci.* **26**, 798.
Michalsky, J. J., Stokes, R. A., Avery, R. W. & DeMarcus, W. C. (1974) *Icarus* **21**, 55.
Minton, R. B. (1972) *Comm. Lunar Planet. Lab.* **9**, **339**.
Moroz, V. I. & Cruikshank, D. P. (1969) *J. Atmos. Sci.* **26**, 865.
Morozhenko, A. V. & Yanovitskii, E. G. (1973) *Icarus* **18**, 583.
Munch, G. & Younkin, R. L. (1964) *Astr. J.* **69**, 553.
Newburn Jr, R. L. & Gilkis, S. (1973) *Sp. Sci. Rev.* **14**, 179.
Orton, G. S. (1975) *Icarus* **26**, 159.
Owen, T. (1969) *Icarus* **10**, 355.
Owen, T. & Mason, H. P. (1969) *J. Atmos. Sci.* **26**, 870.
Owen, T. & Westphal, J. A. (1972) *Icarus* **16**, 392.
Pilcher, C. B. & McCord, T. B. (1971) *Ap. J.* **165**, 195.
Pilcher, C. B., Prinn, R. G. & McCord, T. B. (1973) *J. Atmos. Sci.* **30**, 302.
Pilcher, C. B., & Kunkle, T. D. (1976) *Icarus* **27**, 407.
Regas, J. L., Giver, L. P., Boese, P. W. & Miller, J. F. (1975) *Icarus* **24**, 11.
Schorn R. A., Gray, L. D. & Barker, E. S. (1969) *Icarus* **10**, 241.
Schorn R. A. J., Woszczyk, A. & Young, L. D. G. (1975) *Icarus* **25**, 64.
Schorn, R. A., Young, A. T. & Young, L. D. G. (1979) *Icarus* **38**, 428.
Sekera, Z. (1966a) *Memorandum RM-4951-PR*, Rand Corpn (Santa Monica, Calif.).
Sekera, Z. (1966b) *Memorandum RM-5056-PR* Rand Corpn (Santa Monica, Calif.).
Smith, W. H., Macy, W. & Cochran, W. (1980) *Icarus* 42, 93.
Sobolev, V. V. (1963) *A Treatise on Radiative Transfer*, Van Nostrand.

Sobolev, V. V. (1972) *Sov. Astr.* **16**, 324.
Sobolev, V. V. (1975) *Light Scattering in Planetary Atmospheres*, Pergamon Press.
Spinrad, H. (1962) *Publ. astr. Soc. Pacific* **74**, 187.
Teifel, V. G. (1966) *Astr. Zh.* **43**, 154.
Teifel, V. G. (1969) *J. Atmos. Sci.* **26**, 854.
Teifel, V. G. (1976) in *Jupiter* (ed : T. Gehrels), University of Arizona Press, Tucson, p. 441.
Teifel, V. G. (1977a) *Sov. Astr.* **21**, 100.
Teifel, V. G. (1977b) *Icarus* **30**, 138.
Ueno, S. (1960), *Ap. J.* **132**, 729.
van de Hult. H. C. (1952) in *The Atmospheres of the Earth and Planets* (ed : G. P. Kuiper) University of Chicago Press.
van de Hulst, H. C. (1957) *Light Scattering by Small Particles*, Wiley.
van de Hulst, H. C. (1980) *Multiple Light Scattering*, Vol. 2, Academic Press.
Walker, M. F. & Hayes, S. (1967) *Publ. astr. Soc. Pacific* **79**, 464.
West R. A. (1979a,b) *Icarus* **38**, 12, 34.
Wolstencroft, R. D. & Smith, R. J. (1979) *Icarus* **38**, 155.
Young, K. A. & Margolis, J. S. (1977) *Icarus* **30**, 129.
Young, L. D. G. (1972) *Icarus* **12**, 632.
Young, L. D. G. (1974) in *Exploration of the Planetary System* (eds : A. Woszczyk & C. Iwanizewska), D. Reidel.
Young, L. D. G. & Kattawar, G. W. (1976) *Icarus* **29**, 483.
Young, L. D. G. & Kattawar, G. W. (1977) *Icarus* **30**, 360.
Young, L. D. G., Schorn, R. A. J. & Young, A. T. (1980) *Icarus* **41**, 309.
Young, L. D. G., Young A. T. & Woszcyk, A. (1975) *Icarus* **25**, 239.
Young, L. D. G., Young A. T., Young, J. W. & Bergstralah, J. T. (1973) *Ap. J.* **181**, 25.